

MIT OpenCourseWare
<http://ocw.mit.edu>

Haus, Hermann A., and James R. Melcher. *Electromagnetic Fields and Energy*. Englewood Cliffs, NJ: Prentice-Hall, 1989. ISBN: 9780132490207.

Please use the following citation format:

Haus, Hermann A., and James R. Melcher, *Electromagnetic Fields and Energy*. (Massachusetts Institute of Technology: MIT OpenCourseWare). <http://ocw.mit.edu> (accessed MM DD, YYYY). Also available from Prentice-Hall: Englewood Cliffs, NJ, 1989. ISBN: 9780132490207. License: Creative Commons Attribution-Noncommercial-Share Alike.

Note: Please use the actual date you accessed this material in your citation.

For more information about citing these materials or our Terms of Use, visit:
<http://ocw.mit.edu/terms>

ONE-DIMENSIONAL WAVE DYNAMICS

14.0 INTRODUCTION

Examples of conductor pairs range from parallel conductor transmission lines carrying gigawatts of power to coaxial lines carrying microwatt signals between computers. When these lines become very long, times of interest become very short, or frequencies become very high, electromagnetic wave dynamics play an essential role. The transmission line model developed in this chapter is therefore widely used.

Equally well described by the transmission line model are plane waves, which are often used as representations of radiation fields at radio, microwave, and optical frequencies. For both qualitative and quantitative purposes, there is again a need to develop convenient ways of analyzing the dynamics of such systems. Thus, there are practical reasons for extending the analysis of TEM waves and one-dimensional plane waves given in Chap. 13.

The wave equation is ubiquitous. Although this equation represents most accurately electromagnetic waves, it is also applicable to acoustic waves, whether they be in gases, liquids or solids. The dynamic interaction between excitation amplitudes (E and H fields in the electromagnetic case, pressure and velocity fields in the acoustic case) is displayed very clearly by the solutions to the wave equation. The developments of this chapter are therefore an investment in understanding other more complex dynamic phenomena.

We begin in Sec. 14.1 with the distributed parameter ideal transmission line. This provides an exact representation of plane (one-dimensional) waves. In Sec. 14.2, it is shown that for a wide class of two-conductor systems, uniform in an axial direction, the transmission line equations provide an exact description of the TEM fields. Although such fields are in general three dimensional, their propagation in the axial direction is exactly represented by the one-dimensional wave equation to the extent that the conductors and insulators are perfect. The distributed parameter

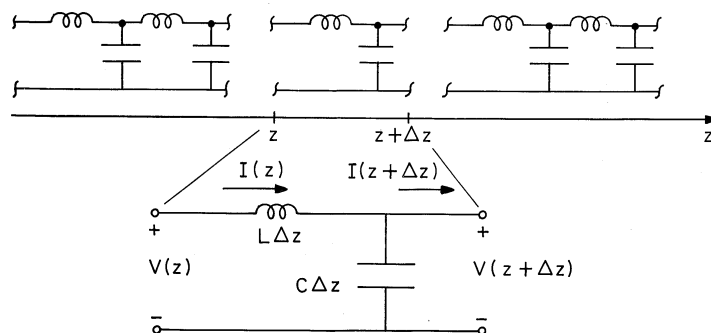


Fig. 14.1.1 Incremental length of distributed parameter transmission line.

model is also commonly used in an approximate way to describe systems that do not support fields that are exactly TEM.

Sections 14.3–14.6 deal with the space-time evolution of transmission line voltage and current. Sections 14.3–14.4, which concentrate on the transient response, are especially applicable to the propagation of digital signals. Sections 14.5–14.6 concentrate on the sinusoidal steady state that prevails in power transmission and communication systems.

The effects of electrical losses on electromagnetic waves, propagating through lossy media or on lossy structures, are considered in Secs. 14.7–14.9. The distributed parameter model is generalized to include the electrical losses in Sec. 14.7. A limiting form of this model provides an “exact” representation of TEM waves in lossy media, either propagating in free space or along pairs of perfect conductors embedded in uniform lossy media. This limit is developed in Sec. 14.8. Once the conductors are taken as being “perfect,” the model is exact and the model is equivalent to the physical system. However, a second limit of the lossy transmission line model, which is exemplified in Sec. 14.9, is not “exact.” In this case, conductor losses give rise to an electric field in the direction of propagation. Thus, the fields are not TEM and this section gives a more realistic view of how quasi-one-dimensional models are often used.

14.1 DISTRIBUTED PARAMETER EQUIVALENTS AND MODELS

The theme of this section is the *distributed parameter transmission line* shown in Fig. 14.1.1. Over any finite axial length of interest, there is an infinite set of the basic units shown in the inset, an infinite number of capacitors and inductors. The parameters L and C are defined per unit length. Thus, for the segment shown between $z + \Delta z$ and z , $L\Delta z$ is the series inductance (in Henrys) of a section of the distributed line having length Δz , while $C\Delta z$ is the shunt capacitance (in Farads).

In the limit where the incremental length $\Delta z \rightarrow 0$, this distributed parameter transmission line serves as a model for the propagation of three types of electromagnetic fields.¹

¹ To facilitate comparison with quasistatic fields, the direction of wave propagation for TEM waves in Chap. 13 was taken as y . It is more customary to make it z .

- First, it gives an exact representation of uniformly polarized electromagnetic plane waves. Whether these are waves in free space, perhaps as launched by the dipole considered in Sec. 12.2, or TEM waves between plane parallel perfectly conducting electrodes, Sec. 13.1, these fields depend only on one spatial coordinate and time.
- Second, we will see in the next section that the distributed parameter transmission line represents exactly the (z, t) dependence of TEM waves propagating on pairs of axially uniform perfect conductors forming transmission lines of arbitrary cross-section. Such systems are a generalization of the parallel plate transmission line. By contrast with that special case, however, the fields generally depend on the transverse coordinates. These fields are therefore, in general, three dimensional.
- Third, it represents in an approximate way, the (z, t) dependence for systems of large aspect ratio, having lengths over which the fields evolve in the z direction (e.g., wavelengths) that are long compared to the transverse dimensions. To reflect the approximate nature of the model and the two- or three-dimensional nature of the system it represents, it is sometimes said to be *quasi-one-dimensional*.

We can obtain a pair of partial differential equations governing the transmission line current $I(z, t)$ and voltage $V(z, t)$ by first requiring that the currents into the node of the elemental section sum to zero

$$I(z) - I(z + \Delta z) = C\Delta z \frac{\partial V}{\partial t} \quad (1)$$

and then requiring that the series voltage drops around the circuit also sum to zero.

$$V(z) - V(z + \Delta z) = L\Delta z \frac{\partial I}{\partial t} \quad (2)$$

Then, division by Δz and recognition that

$$\lim_{\Delta z \rightarrow 0} \frac{f(z + \Delta z) - f(z)}{\Delta z} = \frac{\partial f}{\partial z} \quad (3)$$

results in the *transmission line equations*.

$$\boxed{\frac{\partial I}{\partial z} = -C \frac{\partial V}{\partial t}} \quad (4)$$

$$\boxed{\frac{\partial V}{\partial z} = -L \frac{\partial I}{\partial t}} \quad (5)$$

The remainder of this section is an introduction to some of the physical situations represented by these laws.

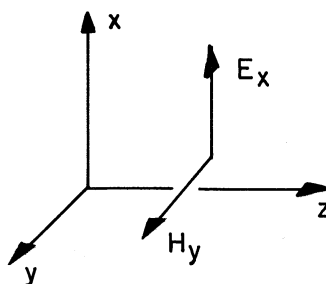


Fig. 14.1.2 Possible polarization and direction of propagation of plane wave described by the transmission line equations.

Plane-Waves. In the following sections, we will develop techniques for describing the space-time evolution of fields on transmission lines. These are equally applicable to the description of electromagnetic plane waves. For example, suppose the fields take the form shown in Fig. 14.1.2.

$$\mathbf{E} = E_x(z, t)\mathbf{i}_x; \quad \mathbf{H} = H_y(z, t)\mathbf{i}_y \quad (6)$$

Then, the x and y components of the laws of Ampère and Faraday reduce to²

$$-\frac{\partial H_y}{\partial z} = \epsilon \frac{\partial E_x}{\partial t} \quad (7)$$

$$\frac{\partial E_x}{\partial z} = -\mu \frac{\partial H_y}{\partial t} \quad (8)$$

These laws are identical to the transmission line equations, (4) and (5), with

$$H_y \leftrightarrow I, \quad E_x \leftrightarrow V, \quad \epsilon \leftrightarrow C, \quad \mu \leftrightarrow L \quad (9)$$

With this identification of variables and parameters, the discussion is equally applicable to plane waves, whether we are considering wave transients or the sinusoidal steady state in the following sections.

Ideal Transmission Line. The TEM fields that can exist between the parallel plates of Fig. 14.1.3 can either be regarded as plane waves that happen to meet the boundary conditions imposed by the electrodes or as a special case of transmission line fields. The following example illustrates the transition to the second viewpoint.

Example 14.1.1. Plane Parallel Plate Transmission Line

In this case, the fields E_x and H_y pictured in Fig. 14.1.2 and described by (7) and (8) can exist unaltered between the plates of Fig. 14.1.3. If the voltage and current are defined as

$$V = E_x a; \quad I = H_y w \quad (10)$$

² Compare with (13.1.2) and (13.1.3) for fields in $x - z$ plane and propagating in the y direction.

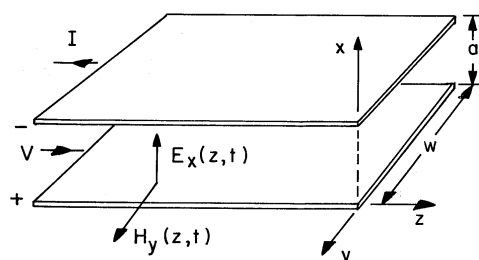


Fig. 14.1.3 Example of transmission line where conductors are parallel plates.

Equations (7) and (8) become identical to the transmission line equations, (4) and (5), with the capacitance and inductance per unit length defined as

$$C = \frac{w\epsilon}{a}; \quad L = \frac{a\mu}{w} \quad (11)$$

Note that these are indeed the C and L that would be found in Chaps. 5 and 8 for the pair of perfectly conducting plates shown in Fig. 14.1.3 if they had unit length in the z direction and were, respectively, “open circuited” and “short circuited” at the right end.

As an alternative to a field description, the distributed $L-C$ transmission line model gives circuit theory interpretation to the physical processes at work in the actual system. As expressed by (1) and hence (4), the current I can be a function of z because some of it can be diverted into charging the “capacitance” of the line. This is an alternative way of representing the effect of the displacement current density on the right in Ampère’s law, (7). The voltage V is a function of z because the inductance of the line causes a voltage drop, even though the conductors are pictured as having no resistance. This follows from (2) and (5) and embodies the same information as did Faraday’s differential law (8). The integral of \mathbf{E} from one conductor to the other at some location z can differ from that at another location because of the flux linked by a contour consisting of these integration paths and closing by contours along the perfect conductors.

In the next section, we will generalize our picture of TEM waves and see that (4) and (5) *exactly* describe transverse waves on pairs of perfect conductors of arbitrary cross-section. Of course, L and C are the inductance per unit length and capacitance per unit length of the particular conductor pair under consideration. The fields depend not only on the independent variables (z, t) appearing explicitly in the transmission line equations, but upon the transverse coordinates as well. Thus, the parallel plate transmission line and the generalization of that line considered in the next section are examples for which the distributed parameter model is exact.

In these cases, TEM waves are exact solutions to the boundary value problem at all frequencies, including frequencies so high that the wavelength of the TEM wave is comparable to, or smaller than, the transverse dimensions of the line. As one would expect from the analysis of Secs. 13.1–13.3, higher-order modes propagating in the z direction are also valid solutions. These are not described by the transmission line equations (4) and (5).

Quasi-One-Dimensional Models. The distributed parameter model is also often used to represent fields that are *not quite* TEM. As an example where an approximate model consists of the distributed $L - C$ network, suppose that the region between the plane parallel plate conductors is filled to the level $x = d < a$ by a dielectric of one permittivity with the remainder filled by a material having a different permittivity. The region between the conductors is then one of nonuniform permittivity. We would find that it is not possible to exactly satisfy the boundary conditions on both the tangential and normal electric fields at the interface between dielectrics with an electric field that only had components transverse to z .³ Even so, if the wavelength is very long compared to the transverse dimensions, the distributed parameter model provides a useful approximate description. The capacitance per unit length used in this model reflects the effect of the nonuniform dielectric in an approximate way.

14.2 TRANSVERSE ELECTROMAGNETIC WAVES

The parallel plates of Sec. 13.1 are a special case of the general configuration shown in Fig. 14.2.1. The conductors have the same cross-section in any plane $z = \text{constant}$, but their cross-sectional geometry is arbitrary.⁴ The region between the pair of perfect conductors is filled by a material having uniform permittivity ϵ and permeability μ . In this section, we show that such a structure can support fields that are transverse to the axial coordinate z , and that the $z - t$ dependence of these fields is described by the ideal transmission line model.

Two common transmission line configurations are illustrated in Fig. 14.2.2.

The TEM fields are conveniently pictured in terms of the vector and scalar potentials, \mathbf{A} and Φ , generalized to describe electrodynamic fields in Sec. 12.1. This is because such fields have only an axial component of \mathbf{A} .

$$\mathbf{A} = A_z(x, y, z, t)\mathbf{i}_z \quad (1)$$

Indeed, evaluation in Cartesian coordinates, shows that even though A_z is in general not only a function of the transverse coordinates but of the axial coordinate z as well, there is no longitudinal component of \mathbf{H} .

To insure that the electric field is also transverse to the z axis, the z component of the expression relating \mathbf{E} to \mathbf{A} and Φ (12.1.3) must be zero.

$$E_z = -\frac{\partial\Phi}{\partial z} - \frac{\partial A_z}{\partial t} = 0 \quad (2)$$

A second relation between Φ and A_z is the gauge condition, (12.1.7), which in view of (1) becomes

$$\frac{\partial A_z}{\partial z} = -\mu\epsilon \frac{\partial\Phi}{\partial t} \quad (3)$$

³ We can see that a uniform plane wave cannot describe such a situation because the propagational velocities of plane waves in dielectrics of different permittivities differ.

⁴ The direction of propagation is now z rather than y .

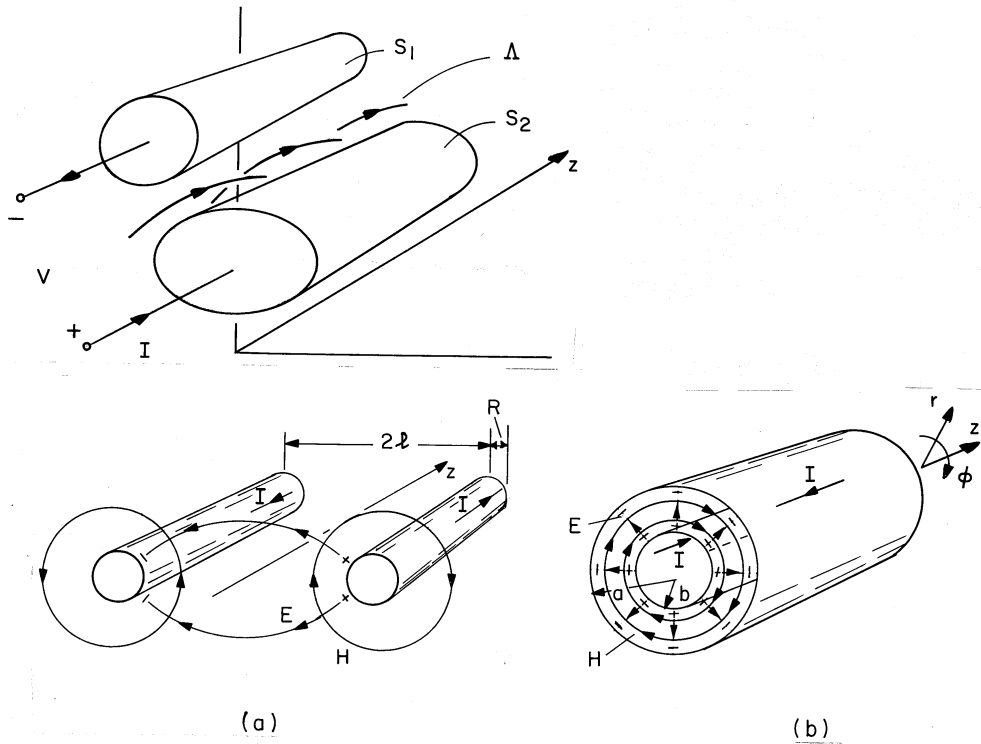


Fig. 14.2.1 Configuration of two parallel perfect conductors supporting TEM fields.

Fig. 14.2.2 Two examples of transmission lines that support TEM waves: (a) parallel wire conductors; and (b) coaxial conductors.

These last two equations combine to show that both Φ and A_z must satisfy

the one-dimensional wave equation. For example, elimination of $\partial^2 A_z / \partial z \partial t$ between the z derivative of (2) and the time derivative of (3) gives

$$\frac{\partial^2 \Phi}{\partial z^2} = \mu\epsilon \frac{\partial^2 \Phi}{\partial t^2} \quad (4)$$

A similar manipulation, with the roles of z and t reversed, shows that A_z also satisfies the one-dimensional wave equation.

$$\frac{\partial^2 A_z}{\partial z^2} = \mu\epsilon \frac{\partial^2 A_z}{\partial t^2} \quad (5)$$

Even though the potentials satisfy the one-dimensional wave equations, in general they depend on the transverse coordinates. In fact, the differential equation governing the dependence on the transverse coordinates is the two-dimensional Laplace's equation. To see this, observe that the three-dimensional Laplacian consists of a part involving derivatives with respect to the transverse coordinates and a second derivative with respect to z .

$$\nabla^2 = \nabla_T^2 + \frac{\partial^2}{\partial z^2} \quad (6)$$

In general, Φ and \mathbf{A} satisfy the three-dimensional wave equation, the homogeneous forms of (12.1.8) and (12.1.10). But, in view of (4) and (5), these expressions reduce to

$$\nabla_T^2 \Phi = 0 \quad (7)$$

$$\nabla_T^2 A_z = 0 \quad (8)$$

where the Laplacian ∇_T^2 is the two-dimensional Laplacian, written in terms of the transverse coordinates.

Even though the fields actually depend on z , *the transverse dependence is as though the fields were quasistatic and two dimensional.*

The boundary conditions on the surfaces of the conductors require that there be no tangential \mathbf{E} and no normal \mathbf{B} . The latter condition prevails if A_z is constant on the surfaces of the conductors. This condition is familiar from Sec. 8.6. With A_z defined as zero on the surface S_1 of one of the conductors, as shown in Fig. 14.2.1, it is equal to the flux per unit length passing between the conductors when evaluated anywhere on the second conductor. Thus, the boundary conditions imposed on A_z are

$$A_z = 0 \text{ on } S_1; \quad A_z = \Lambda(z, t) \text{ on } S_2 \quad (9)$$

As described in Sec. 8.6, where two-dimensional magnetic fields were represented in terms of A_z , Λ is the flux per unit length passing between the conductors. Because \mathbf{E} is transverse to z and \mathbf{A} has only a z component, \mathbf{E} is found from Φ by taking the transverse gradient just as if the fields were two dimensional. The boundary condition on \mathbf{E} , met by making Φ constant on the surfaces of the conductors, is therefore familiar from Chaps. 4 and 5.

$$\Phi = 0 \text{ on } S_1; \quad \Phi = V(z, t) \text{ on } S_2 \quad (10)$$

By definition, Λ is equal to the inductance per unit length L times the total current I carried by the conductor having the surface S_2 .

$$\Lambda = LI \quad (11)$$

The first of the transmission line equations is now obtained simply by evaluating (2) on the boundary S_2 of the second conductor and using the definition of Λ from (11).

$$\boxed{\frac{\partial V}{\partial z} + L \frac{\partial I}{\partial t} = 0} \quad (12)$$

The second equation follows from a similar evaluation of (3). This time we introduce the capacitance per unit length by exploiting the relation $LC = \mu\epsilon$, (8.6.14).

$$\boxed{\frac{\partial I}{\partial z} + C \frac{\partial V}{\partial t} = 0} \quad (13)$$

The integral of \mathbf{E} between the conductors within a given plane of constant z is V , and can be interpreted as the voltage between the two conductors. The total current carried in the $+z$ direction through a plane of constant z by one of the conductors and returned in the $-z$ direction by the other is I . *Because effects of magnetic induction are important, V is a function of z . Similarly, because the displacement current is important, the current I is also a function of z .*

Example 14.2.1. Parallel Plate Transmission Line

Between the perfectly conducting parallel plates of Fig. 14.1.3, solutions to (7) and (8) that meet the boundary conditions of (9) and (10) are

$$A_z = \Lambda(z, t) \left(1 - \frac{x}{a}\right) = \frac{a\mu}{w} \left(1 - \frac{x}{a}\right) I(z, t) \quad (14)$$

$$\Phi = \left(1 - \frac{x}{a}\right) V(z, t) \quad (15)$$

In the EQS context of Chap. 5, the latter is the potential associated with a uniform electric field between plane parallel electrodes, while in the MQS context of Example 8.4.4, (14) is the vector potential associated with the uniform magnetic field inside a one-turn solenoid. The inductance per unit length follows from (11) and the evaluation of (14) on the surface S_2 , and one way to evaluate the capacitance per unit length is to use the relation $LC = \mu\epsilon$.

$$L = \frac{\mu a}{w}; \quad C = \frac{\mu\epsilon}{L} = \frac{\epsilon w}{a} \quad (16)$$

Every two-dimensional example from Chap. 4 with perfectly conducting boundaries is a candidate for supporting TEM fields that propagate in a direction perpendicular to the two dimensions. For every solution to (7) meeting the boundary

conditions of (10), there is one to (8) satisfying the conditions of (9). This follows from the antiduality exploited in Chap. 8 to describe the magnetic fields with perfectly conducting boundaries (Example 8.6.3). The next example illustrates how we can draw upon results from these earlier chapters.

Example 14.2.2. Parallel Wire Transmission Line

For the parallel wire configuration of Fig. 14.2.2a, the capacitance per unit length was derived in Example 4.6.3, (4.6.27).

$$C = \frac{\pi\epsilon}{\ln\left[\frac{l}{R} + \sqrt{\left(\frac{l}{R}\right)^2 - 1}\right]} \quad (17)$$

The inductance per unit length was derived in Example 8.6.1, (8.6.12).

$$L = \frac{\mu}{\pi} \ln\left[\frac{l}{R} + \sqrt{\left(\frac{l}{R}\right)^2 - 1}\right] \quad (18)$$

Of course, the product of these is $\mu\epsilon$.

At any given instant, the electric and magnetic fields have a cross-sectional distribution depicted by Figs. 4.6.5 and 8.6.6, respectively. The evolution of the fields with z and t are predicted by the one-dimensional wave equation, (4) or (5), or a similar equation resulting from combining the transmission line equations.

Propagation is in the z direction. With the understanding that the fields have transverse distributions that are identical to the EQS and MQS patterns, the next sections focus on the evolution of the fields with z and t .

No TEM Fields in Hollow Pipes. From the general description of TEM fields given in this section, we can see that TEM modes will not exist inside a hollow perfectly conducting pipe. This follows from the fact that both A_z and Φ must be constant on the walls of such a pipe, and solutions to (7) and (8) that meet these conditions are that A_z and Φ , respectively, are equal to these constants throughout. From Sec. 5.2, we know that these solutions to Laplace's equation are unique. The \mathbf{E} and \mathbf{H} they represent are zero, so there can be no TEM fields. This is consistent with the finding for rectangular waveguides in Sec. 13.4. The parallel plate configuration considered in Secs. 13.1–13.3 could support TEM modes because it was assumed that in any given cross-section (perpendicular to the axial position), the electrodes were insulated from each other.

Power-flow and Energy Storage. The transmission line model expresses the fields in terms of V and I . For the TEM fields, this is not an approximation but rather an elegant way of dealing with a class of three-dimensional time-dependent fields. To emphasize this point, we now show the equivalence of power flow and energy storage as derived from the transmission line model and from Poynting's theorem.

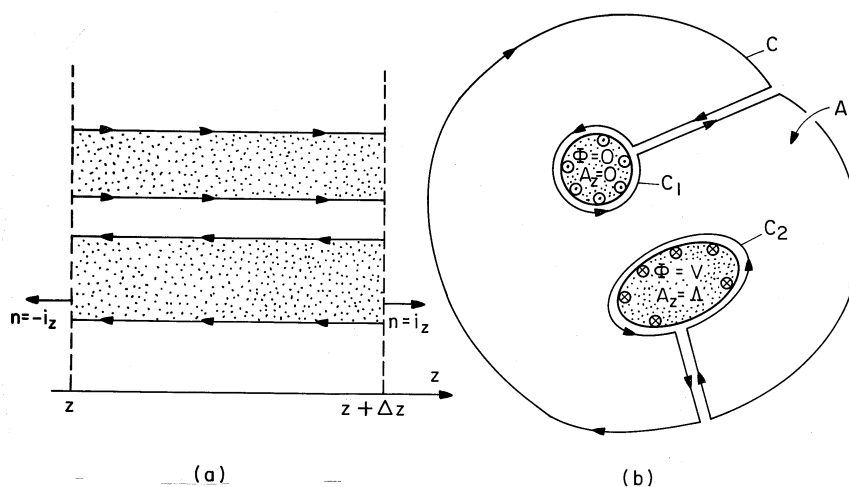


Fig. 14.2.3 Incremental length of transmission line and its cross-section.

An incremental length, Δz , of a two-conductor system and its cross-section are pictured in Fig. 14.2.3. A one-dimensional version of the energy conservation law introduced in Sec. 11.1 can be derived from the transmission line equations using manipulations analogous to those used to derive Poynting's theorem in Sec. 11.2. We multiply (14.1.4) by V and (14.1.5) by I and add. The result is a one-dimensional statement of energy conservation.

$$-\frac{\partial}{\partial z}(VI) = \frac{\partial}{\partial t}\left(\frac{1}{2}CV^2 + \frac{1}{2}LI^2\right) \quad (19)$$

This equation has intuitive "appeal." The power flowing in the z direction is VI , and the energy per unit length stored in the electric and magnetic fields is $\frac{1}{2}CV^2$ and $\frac{1}{2}LI^2$, respectively. Multiplied by Δz , (19) states that the amount by which the power flow at z exceeds that at $z + \Delta z$ is equal to the rate at which energy is stored in the length Δz of the line.

We can obtain the same result from the three-dimensional Poynting's integral theorem, (11.1.1), evaluated using (11.3.3), and applied to a volume element of incremental length Δz but one having the cross-sectional area A of the system (if need be, one extending to infinity).

$$\begin{aligned} & -\left[\int_A \mathbf{E} \times \mathbf{H} \cdot \mathbf{i}_z da|_{z+\Delta z} - \int_A \mathbf{E} \times \mathbf{H} \cdot \mathbf{i}_z da|_z\right] \\ & = \frac{\partial}{\partial t} \int_A \left(\frac{1}{2}\epsilon \mathbf{E} \cdot \mathbf{E} + \frac{1}{2}\mu \mathbf{H} \cdot \mathbf{H}\right) da \Delta z \end{aligned} \quad (20)$$

Here, the integral of Poynting's flux density, $\mathbf{E} \times \mathbf{H}$, over a closed surface S has been converted to one over the cross-sectional areas A in the planes z and $z + \Delta z$. The closed surface is in this case a cylinder having length Δz in the z direction

and a lateral surface described by the contour C in Fig. 14.2.3b. The integrals of Poynting's flux density over the various parts of this lateral surface (having circumference C and length Δz) either are zero or cancel. For example, on the surfaces of the conductors denoted by C_1 and C_2 , the contributions are zero because \mathbf{E} is perpendicular. Thus, the contributions to the integral over S come only from integrations over A in the planes $z + \Delta z$ and z . Note that in writing these contributions on the left in (20), the normal to S on these surfaces is \mathbf{i}_z and $-\mathbf{i}_z$, respectively.

To see that the integrals of the Poynting flux over the cross-section of the system are indeed simply VI , \mathbf{E} is written in terms of the potentials (12.1.3).

$$\int_A \mathbf{E} \times \mathbf{H} \cdot \mathbf{i}_z da = \int_A \left(-\nabla\Phi - \frac{\partial \mathbf{A}}{\partial t} \right) \times \mathbf{H} \cdot \mathbf{i}_z da \quad (21)$$

The surface of integration has its normal in the z direction. Because \mathbf{A} is also in the z direction, the cross-product of $\partial \mathbf{A} / \partial t$ with \mathbf{H} must be perpendicular to z , and therefore makes no contribution to the integral. A vector identity then converts the integral to

$$\begin{aligned} \int_A \mathbf{E} \times \mathbf{H} \cdot \mathbf{i}_z da &= \int_A -\nabla\Phi \times \mathbf{H} \cdot \mathbf{i}_z da \\ &= - \int_A \nabla \times (\Phi \mathbf{H}) \cdot \mathbf{i}_z da \\ &\quad + \int_A \Phi \nabla \times \mathbf{H} \cdot \mathbf{i}_z da \end{aligned} \quad (22)$$

In Fig. 14.2.3, the area A , enclosed by the contour C , is insulating. Thus, because $\mathbf{J} = 0$ in this region and the electric field, and hence the displacement current, are perpendicular to the surface of integration, Ampère's law tells us that the integrand in the second integral is zero. The first integral can be converted, by Stokes' theorem, to a line integral.

$$\int_A \mathbf{E} \times \mathbf{H} \cdot \mathbf{i}_z da = - \oint_C \Phi \mathbf{H} \cdot d\mathbf{s} \quad (23)$$

On the contour, $\Phi = 0$ on C_1 and at infinity. The contributions along the segments connecting C_1 and C_2 to infinity cancel, and so the only contribution comes from C_2 . On that contour, $\Phi = V$, so Φ is a constant. Finally, again because the displacement current is perpendicular to $d\mathbf{s}$, Ampère's integral law requires that the line integral of \mathbf{H} on the contour C_2 enclosing the conductor having potential V be equal to $-I$. Thus, (23) becomes

$$\int_A \mathbf{E} \times \mathbf{H} \cdot \mathbf{i}_z da = -V \oint_{C_2} \mathbf{H} \cdot d\mathbf{s} = VI \quad (24)$$

The axial power flux pictured by Poynting's theorem as passing through the insulating region between the conductors can just as well be represented by the current and voltage of one of the conductors. To formalize the equivalence of these points of view, (24) is used to evaluate the left-hand side of Poynting's theorem, (20), and that expression divided by Δz .

$$\begin{aligned} &\frac{[V(z + \Delta z)I(z + \Delta z) - V(z)I(z)]}{\Delta z} \\ &= \frac{\partial}{\partial t} \int_A \left(\frac{1}{2} \epsilon \mathbf{E} \cdot \mathbf{E} + \frac{1}{2} \mu \mathbf{H} \cdot \mathbf{H} \right) da \end{aligned} \quad (25)$$

In the limit $\Delta z \rightarrow 0$, this statement is equivalent to that implied by the transmission line equations, (19), because the electric and magnetic energy storages per unit length are

$$\frac{1}{2}CV^2 = \int_A \frac{1}{2}\epsilon \mathbf{E} \cdot \mathbf{E} da; \quad \frac{1}{2}LI^2 = \int_A \frac{1}{2}\mu \mathbf{H} \cdot \mathbf{H} da \quad (26)$$

In summary, for TEM fields, we are justified in thinking of a transmission line as storing energies per unit length given by (26) and as carrying a power VI in the z direction.

14.3 TRANSIENTS ON INFINITE TRANSMISSION LINES

The transient response of transmission lines or plane waves is of interest for time-domain reflectometry and for radar. In these applications, it is the delay and shape of the response to pulse-like signals that provides the desired information. Even more common is the use of pulses to represent digitally encoded information carried by various types of cables and optical fibers. Again, pulse delays and reflections are often crucial, and an understanding of how these are endemic to common communications systems is one of the points in this and the next section.

The next four sections develop insights into dynamic phenomena described by the one-dimensional wave equation. This and the next section are concerned with transients and focus on initial as well as boundary conditions to create an awareness of the key role played by causality. Then, with the understanding that effects of the turn-on transient have died away, the sinusoidal steady state response is considered in Secs. 14.5–14.6,

The evolution of the transmission line voltage $V(z, t)$, and hence the associated TEM fields, is governed by the one-dimensional wave equation. This follows by combining the transmission line equations, (14.1.4)-(5), to obtain one expression for V .

$$\frac{\partial^2 V}{\partial z^2} = \frac{1}{c^2} \frac{\partial^2 V}{\partial t^2}; \quad c \equiv \frac{1}{\sqrt{LC}} = \frac{1}{\sqrt{\mu\epsilon}} \quad (1)$$

This equation has a remarkably general pair of solutions

$$V = V_+(\alpha) + V_-(\beta) \quad (2)$$

where V_+ and V_- are *arbitrary* functions of variables α and β that are defined as particular combinations of the independent variables z and t .

$$\alpha = z - ct \quad (3)$$

$$\beta = z + ct \quad (4)$$

To see that this general solution in fact satisfies the wave equation, it is only necessary to perform the derivatives and substitute them into the equation. To that end, observe that

$$\frac{\partial V_{\pm}}{\partial z} = V'_{\pm}; \quad \frac{\partial V_{\pm}}{\partial t} = \mp cV'_{\pm} \quad (5)$$

where primes indicate the derivative with respect to the argument of the function. Carrying out the same process once more gives the second derivatives required to evaluate the wave equation.

$$\frac{\partial^2 V_{\pm}}{\partial z^2} = V_{\pm}''; \quad \frac{\partial^2 V_{\pm}}{\partial t^2} = c^2 V_{\pm}'' \quad (6)$$

Substitution of these expressions for the derivatives in (1) shows that (1) is satisfied. Functions having the form of (2) are indeed solutions to the wave equation.

According to (2), V is a superposition of fields that propagate, without changing their shape, in the positive and negative z directions. With α maintained constant, the component V_+ is constant. With α a constant, the position z increases with time according to the law

$$z = \alpha + ct \quad (7)$$

The shape of the second component of (2) remains invariant when β is held constant, as it is if the z coordinate decreases at the rate c . The functions $V_+(z - ct)$ and $V_-(z + ct)$ represent forward and backward waves proceeding without change of shape at the speed c in the $+z$ and $-z$ directions respectively. We conclude that the voltage can be represented as a superposition of forward and backward waves, V_+ and V_- , which, if the space surrounding the conductors is free space (where $\epsilon = \epsilon_o$ and $\mu = \mu_o$), propagate with the velocity $c \simeq 3 \times 10^8$ m/s of light.

Because $I(z, t)$ also satisfies the one-dimensional wave equation, it also can be written as the sum of traveling waves.

$$I = I_+(\alpha) + I_-(\beta) \quad (8)$$

The relationships between these components of I and those of V are found by substitution of (2) and (8) into either of the transmission line equations, (14.1.4)–(14.1.5), which give the same result if it is remembered that $c = 1/\sqrt{LC}$. In summary, as fundamental solutions to the equations representing the ideal transmission line, we have

$$\boxed{V = V_+(\alpha) + V_-(\beta)} \quad (9)$$

$$\boxed{I = \frac{1}{Z_o}[V_+(\alpha) - V_-(\beta)]} \quad (10)$$

where

$$\alpha = z - ct; \quad \beta = z + ct \quad (11)$$

Here, Z_o is defined as the *characteristic impedance* of the line.

$$\boxed{Z_o \equiv \sqrt{L/C}} \quad (12)$$

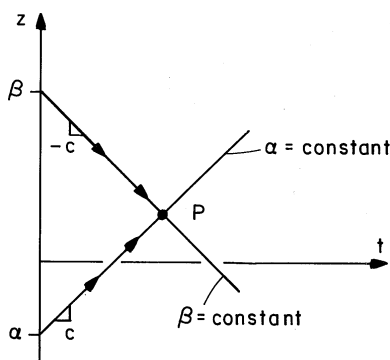


Fig. 14.3.1 Waves initiated at $z = \alpha$ and $z = \beta$ propagate along the lines of constant α and β to combine at P .

Typically, Z_o is the intrinsic impedance $\sqrt{\mu/\epsilon}$ multiplied by a function of the ratio of dimensions describing the cross-sectional geometry of the line.

Illustration. Characteristic Impedance of Parallel Wires

For example, the parallel wire transmission line of Example 14.2.2 has the characteristic impedance

$$\sqrt{L/C} = \frac{1}{\pi} \ln \left[\frac{l}{R} + \sqrt{\left(\frac{l}{R}\right)^2 - 1} \right] \sqrt{\mu/\epsilon} \tag{13}$$

where for free space, $\sqrt{\mu/\epsilon} \approx 377\Omega$.

Response to Initial Conditions. The specification of the distribution of V and I at an initial time, $t = 0$, leads to two traveling waves. It is helpful to picture the field evolution in the $z - t$ plane shown in Fig. 14.3.1. In this plane, the $\alpha = \text{constant}$ and $\beta = \text{constant}$ *characteristic lines* are straight and have slopes $\pm c$, respectively.

When $t = 0$, we are given that along the z axis,

$$V(z, 0) = V_i(z) \tag{14}$$

$$I(z, 0) = I_i(z) \tag{15}$$

What are these fields at some later time, such as at P in Fig. 14.3.1?

We answer this question in two steps. First, we use the initial conditions to establish the separate components V_+ and V_- at each position when $t = 0$. To this end, the initial conditions of (14) and (15) are substituted for the quantities on the left in (9) and (10) to obtain two equations for these unknowns.

$$V_+ + V_- = V_i \tag{16}$$

$$\frac{1}{Z_o}(V_+ - V_-) = I_i \tag{17}$$

These expressions can then be solved for the components in terms of the initial conditions.

$$\boxed{V_+ = \frac{1}{2}(I_i Z_o + V_i)} \quad (18)$$

$$\boxed{V_- = \frac{1}{2}(-I_i Z_o + V_i)} \quad (19)$$

The second step combines these components to determine the field at P in Fig. 14.3.1. Here we use the invariance of V_+ along the line $\alpha = \text{constant}$ and the invariance of V_- along the line $\beta = \text{constant}$. The way in which these components combine at P to give V and I is summarized by (9) and (10). The total voltage at P is the sum of the components, while the current is the characteristic admittance Z_o^{-1} multiplied by the difference of the components.

The following examples illustrate how the initial conditions determine the invariants (the waves V_{\pm} propagating in the $\pm z$ directions) and how these invariants in turn determine the fields at a subsequent time and different position. They show how the response at P in Fig. 14.3.1 is determined by the initial conditions at just two locations, indicated in the figure by the points $z = \alpha$ and $z = \beta$. Implicit in our understanding of the dynamics is causality. The response at the location P at some *later* time is the result of conditions at $(z = \alpha, t = 0)$ that propagate with the velocity c in the $+z$ direction and conditions at $(z = \beta, t = 0)$ that propagate in the $-z$ direction with velocity c .

Example 14.3.1. Initiation of a Pure Traveling Wave

In Example 3.1.1, we were introduced to a uniform plane wave composed of a single component traveling in the $+z$ direction. The particular initial conditions for E_x and H_y [(3.1.9) and (3.1.10)] were selected so that the response would be composed of just the wave propagating in the $+z$ direction. Given that the initial distribution of E_x is

$$E_x(z, 0) = E_i(z) = E_o e^{-z^2/2a^2} \quad (20)$$

can we now show how to select a distribution of H_y such that there is no part of the response propagating in the $-z$ direction?

In applying the transmission line to plane waves, we make the identification (14.1.9)

$$V \leftrightarrow E_x, \quad I \leftrightarrow H_y, \quad C \leftrightarrow \epsilon_o, \quad L \leftrightarrow \mu_o \Rightarrow Z_o \leftrightarrow \sqrt{\frac{\mu_o}{\epsilon_o}} \quad (21)$$

We are assured that $E_- = 0$ by making the right-hand side of (19) vanish. Thus, we make

$$H_i = \sqrt{\frac{\epsilon_o}{\mu_o}} E_i = \sqrt{\frac{\epsilon_o}{\mu_o}} E_o e^{-z^2/2a^2} \quad (22)$$

It follows from (18) and (19) that along the characteristic lines passing through $(z, 0)$,

$$E_+ = E_i; \quad E_- = 0 \quad (23)$$

and from (9) and (10) that the subsequent fields are

$$E_x = E_+ = E_o e^{-(z-ct)^2/2a^2} \quad (24)$$

$$H_y = \sqrt{\frac{\epsilon_o}{\mu_o}} E_+ = \sqrt{\frac{\epsilon_o}{\mu_o}} E_o e^{-(z-ct)^2/2a^2} \quad (25)$$

These are the traveling electromagnetic waves found “the hard way” in Example 3.1.1.

The following example gives further substance to the two-step process used to deduce the fields at P in Fig. 14.3.1 from those at $(z = \alpha, t = 0)$ and $(z = \beta, t = 0)$. First, the components V_+ and V_- , respectively, are deduced at $(z = \alpha, t = 0)$ and $(z = \beta, t = 0)$ from the initial conditions. Because V_+ is invariant along the line $\alpha = \text{constant}$ while V_- is invariant along the line $\beta = \text{constant}$, we can then combine these components to determine the fields at P .

Example 14.3.2. Initiation of a Wave Transient

Suppose that when $t = 0$ there is a uniform voltage V_p between the positions $z = -d$ and $z = d$, but that outside this range, $V = 0$. Further, suppose that initially, $I = 0$ over the entire length of the line.

$$V_i = \begin{cases} V_p; & -d < z < d \\ 0; & z < -d \text{ and } d < z \end{cases} \quad (26)$$

What are the subsequent distributions of V and I ? Once we have found these responses, we will see how such initial conditions might be realized physically.

The initial conditions are given a pictorial representation in Fig. 14.3.2, where $V(z, 0) = V_i$ and $I(z, 0) = I_i$ are shown as the solid and broken distributions when $t = 0$.

It follows from (18) and (19) that

$$V_+ = \begin{cases} 0; & \alpha < -d, d < \alpha \\ \frac{1}{2}V_p; & -d < \alpha < d \end{cases}, \quad V_- = \begin{cases} 0; & \beta < -d, d < \beta \\ \frac{1}{2}V_p; & -d < \beta < d \end{cases} \quad (27)$$

Now that the initial conditions have been used to identify the wave components V_{\pm} , we can use (9) and (10) to establish the subsequent V and I . These are also shown in Fig. 14.3.2 using the axis perpendicular to the $z-t$ plane to represent either $V(z, t)$ (the solid lines) or $I(z, t)$ (the dashed lines). Shown in this figure are the initial and two subsequent field distributions. At point P_1 , both V_+ and V_- are zero, so that both V and I are also zero. At points like P_2 , where the wave propagating from $z = d$ has arrived but that from $z = -d$ has not, V_+ is $V_p/2$ while V_- remains zero. At points like P_3 , neither the wave propagating in the $-z$ direction from $z = d$ or that propagating in the $+z$ direction from $z = -d$ has yet arrived, V_+ and V_- are given by (27), and the fields remain the same as they were initially.

By the time $t = d/c$, the wave transient has resolved itself into two pulses propagating in the $+z$ and $-z$ directions with the velocity c . These pulses consist

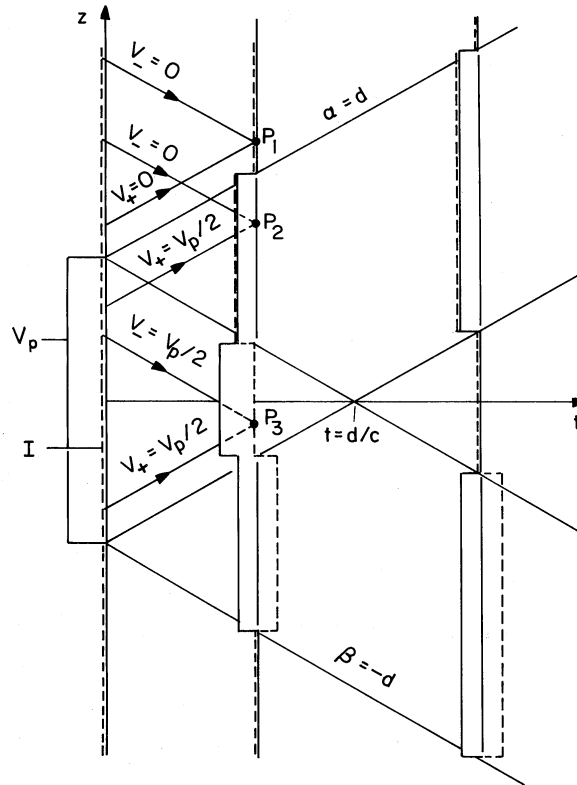


Fig. 14.3.2 Wave transient pictured in the $z - t$ plane. When $t = 0$, $I = 0$ and V assumes a uniform value over the range $-d < z < d$ and is zero outside this range.

of a voltage and a current that are in a constant ratio equal to the characteristic impedance, Z_o .

With the help of the step function $u_{-1}(z)$, defined by

$$u_{-1}(z) \equiv \begin{cases} 0; & z < 0 \\ 1; & 0 < z \end{cases} \quad (28)$$

we can carry out these same steps in analytical terms. The initial conditions are

$$I(z, 0) = 0$$

$$V(z, 0) = V_p[u_{-1}(z + d) - u_{-1}(z - d)] \quad (29)$$

The wave components follow from (18) and (19) and are expressed in terms of the variables α and β because they are invariant along lines where these parameters, respectively, are constant.

$$\begin{aligned} V_+ &= \frac{1}{2}V_p[u_{-1}(\alpha + d) - u_{-1}(\alpha - d)] \\ V_- &= \frac{1}{2}V_p[u_{-1}(\beta + d) - u_{-1}(\beta - d)] \end{aligned} \quad (30)$$

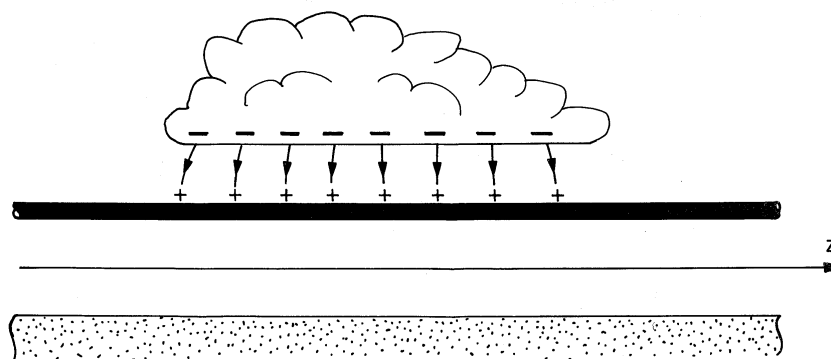


Fig. 14.3.3 Thunderstorm over power line modeled by initial conditions of Fig. 14.3.2.

The voltage and current at the point P in Fig. 14.3.1 follow from substitution of these expressions into (9) and (10). With α and β expressed in terms of (z, t) using (11), it follows that

$$\begin{aligned}
 V &= \frac{1}{2} V_p [u_{-1}(z - ct + d) - u_{-1}(z - ct - d)] \\
 &\quad + \frac{1}{2} V_p [u_{-1}(z + ct + d) - u_{-1}(z + ct - d)] \\
 I &= \frac{1}{2} \frac{V_p}{Z_o} [u_{-1}(z - ct + d) - u_{-1}(z - ct - d)] \\
 &\quad - \frac{1}{2} \frac{V_p}{Z_o} [u_{-1}(z + ct + d) - u_{-1}(z + ct - d)]
 \end{aligned} \tag{31}$$

These are analytical expressions for the the functions depicted by Fig. 14.3.2.

When our lights blink during a thunderstorm, it is possibly due to circuit interruption resulting from a power line transient initiated by a lightning stroke. Even if the discharge does not strike the power line, there can be transients resulting from an accumulation of charge on the line imaging the charge in the cloud above, as shown in Fig. 14.3.3. When the cloud is discharged to ground by the lightning stroke, initial conditions are established that might be modeled by those considered in this example. Just after the lightning discharge, the images for the charge accumulated on the line are on the ground below.

14.4 TRANSIENTS ON BOUNDED TRANSMISSION LINES

Transmission lines are generally connected to a source and to a load, as shown in Fig. 14.4.1a. More complex systems composed of interconnected transmission lines can usually be decomposed into subsystems having this basic configuration. A generator at $z = 0$ is connected to a load at $z = l$ by a transmission line having the length l . In this section, we build upon the traveling wave picture introduced in Sec. 14.3 to describe transients at a boundary initiated by a source.

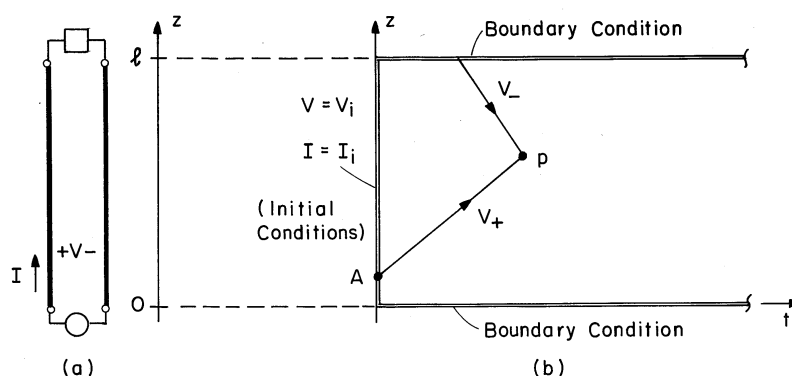


Fig. 14.4.1 (a) Transmission line with terminations. (b) Initial and boundary conditions in $z-t$ plane.

In picturing the evolution with time of the voltage $V(z, t)$ and current $I(z, t)$ on a terminated line, it is again helpful to use the $z-t$ plane shown in Fig. 14.4.1b. The load and generator impose boundary conditions at $z = l$ and $z = 0$. In addition to satisfying these conditions, the distributions of V and I must also satisfy the respective initial values $V = V_i(z)$ and $I = I_i(z)$ when $t = 0$, introduced in Sec. 14.3. Thus, our goal is to find V and I in the \subset -shaped region of $z-t$ space shown in Fig. 14.4.1b.

In Sec. 14.3, we found that the transmission line equations, (14.1.4) and (14.1.5), have solutions

$$V = V_+(\alpha) + V_-(\beta) \quad (1)$$

$$I = \frac{1}{Z_o} [V_+(\alpha) - V_-(\beta)] \quad (2)$$

where

$$\alpha = z - ct; \quad \beta = z + ct \quad (3)$$

and $c = 1/\sqrt{LC}$ and $Z_o = \sqrt{L/C}$.

A mathematical way of saying that V_+ and V_- , respectively, represent waves traveling in the $+z$ and $-z$ directions is to say that these quantities are invariants on the characteristic lines $\alpha = \text{constant}$ and $\beta = \text{constant}$ in the $z-t$ plane.

There are two steps in finding V and I .

- First, the initial conditions, and now the boundary conditions as well, are used to determine V_+ and V_- along the two families of characteristic lines in the region of the $z-t$ plane of interest. This is done with the understanding that causality prevails in the sense that the dynamics evolve in the “direction” of increasing time. Thus it is where a characteristic line enters the \subset -shaped region of Fig. 14.4.1b and goes to the right that the invariant for that line is set.
- Second, the solution at a given point of intersection for the lines $\alpha = \text{constant}$ and $\beta = \text{constant}$ are found in accordance with (1) and (2). This second step can be pictured as in Fig. 14.4.1b. In physical terms, the total voltage or

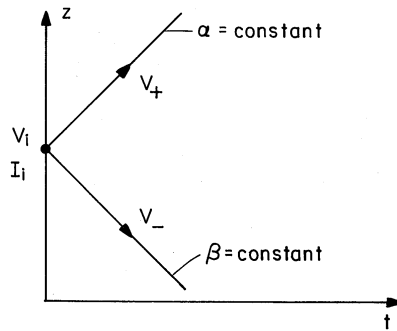


Fig. 14.4.2 Characteristic lines originating on initial conditions.

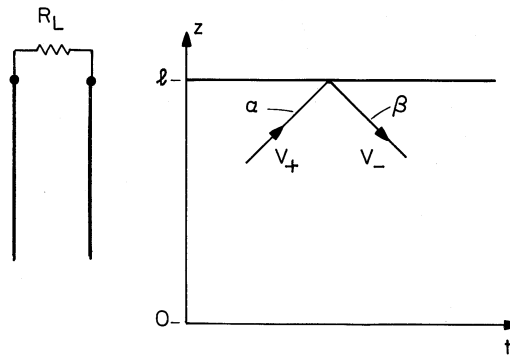


Fig. 14.4.3 Characteristic line originating on load.

current is the superposition of traveling waves propagating along the characteristic lines that intersect at the point of interest.

To complete the first step, note that a characteristic line passing through a given point P has three possible origins. First, it can originate on the $t = 0$ axis, in which case the invariants, V_{\pm} , are determined by the initial conditions. This was the only possibility on the infinite transmission line considered in Sec. 14.3. The initial voltage and current where the characteristic line originates when $t = 0$ in Fig. 14.4.2 is used to evaluate (1) and (2), and the simultaneous solution of these expressions then gives the desired invariants.

$$V_+ = \frac{1}{2}(V_i + Z_o I_i) \tag{4}$$

$$V_- = \frac{1}{2}(V_i - Z_o I_i) \tag{5}$$

The second origin of a characteristic line is the boundary at $z = l$, as shown in Fig. 14.4.3. In particular, we consider the load resistance R_L as the termination that imposes the boundary condition

$$V(l, t) = R_L I(l, t) \tag{6}$$

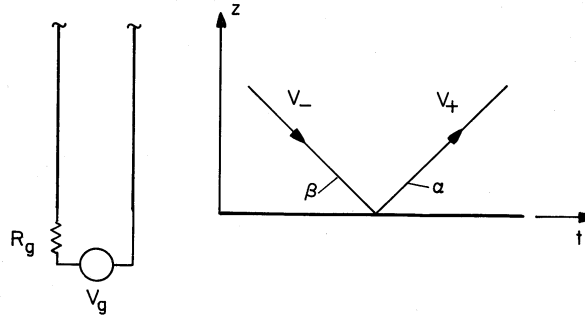


Fig. 14.4.4 Characteristic lines originating on generator end of line.

The problems will illustrate how the same approach illustrated here can also be used to describe terminations composed of arbitrary circuits. Certainly, the case where the load is a pure resistance is the most important type of termination, for reasons that will be clear shortly.

Again, because phenomena proceed in the $+t$ “direction,” the incident wave V_+ and the boundary condition at $z = l$ conspire to determine the reflected wave V_- on the characteristic line $\beta = \text{constant}$ originating on the boundary at $z = l$ (Fig. 14.4.3). To say this mathematically, we substitute (1) and (2) into (6)

$$V_+ + V_- = \frac{R_L}{Z_o}(V_+ - V_-) \quad (7)$$

and solve for V_- .

$$V_- = V_+ \Gamma_L; \quad \Gamma_L \equiv \frac{\left(\frac{R_L}{Z_o} - 1\right)}{\left(\frac{R_L}{Z_o} + 1\right)} \quad (8)$$

Here, V_+ and V_- are evaluated at $z = l$, and hence with $\alpha = l - ct$ and $\beta = l + ct$. Given the incident wave V_+ , we multiply it by the *reflection coefficient* Γ_L and determine V_- .

The third possible origin of a characteristic line passing through the given point P is on the boundary at $z = 0$, as shown in Fig. 14.4.4. Here the line has been terminated in a source modeled as an ideal voltage source, $V_g(t)$, in series with a resistance R_g . In this case, it is the wave traveling in the $-z$ direction (represented by V_- and incident on the boundary from the left in Fig. 14.4.4) that combines with the boundary condition there to determine the reflected wave V_+ .

The boundary condition is the constraint of the circuit on the voltage and current at the terminals.

$$V(0, t) = V_g - R_g I(0, t) \quad (9)$$

Substitution of (1) and (2) then gives an expression that can be solved for V_+ , given V_- and $V_g(t)$.

$$V_+ = \frac{V_g}{\frac{R_g}{Z_o} + 1} + V_- \Gamma_g; \quad \Gamma_g \equiv \frac{\left(\frac{R_g}{Z_o} - 1\right)}{\left(\frac{R_g}{Z_o} + 1\right)} \quad (10)$$

The following examples illustrate the two steps necessary to determine the transient response. First, V_{\pm} are found over the range of time of interest using the initial conditions [(4) and (5) and Fig. 14.4.2] and boundary conditions [(8) and Fig. 14.4.3 and (10) and Fig. 14.4.4]. Then, the wave-components are superimposed to find V and I ((1) and (2) and Fig. 14.4.1.) To appreciate the space-time significance of the equations used in this process, it is helpful to have in mind the associated $z - t$ sketches.

Matching. The reflection of waves from the terminations of a line results in responses that can persist long after a signal has propagated the length of the transmission line. As a practical matter, it is therefore often desirable to eliminate reflections by *matching* the line.

From (8), it follows that wave reflection is eliminated at the load by making the load resistance equal to the characteristic impedance of the line, $R_L = Z_o$. Similarly, from (10), there will be no reflection of the wave V_- at the source if the resistance R_g is made equal to Z_o .

Consider first an example in which the response is made simple because the line is matched to its load.

Example 14.4.1. Matching

In the configuration shown in Fig. 14.4.5a, the load has a resistance R_L while the generator is an ideal voltage source $V_g(t)$ in series with the resistor R_g . The load is matched to the line, $R_L = Z_o$. As a result, according to (8), there are no V_- waves on characteristics originating at the load.

$$R_L = Z_o \Rightarrow V_- = 0 \quad (11)$$

Suppose that the driving voltage consists of a pulse of amplitude V_p and duration T , as shown in Fig. 14.4.5b. Further, suppose that when $t = 0$ the line voltage and current are both zero, $V_i = 0$, and $I_i = 0$. Then, it follows from (4) and (5) that V_+ and V_- are both zero on the respective characteristic lines originating on the $t = 0$ axis, as shown in Fig. 14.4.5b. By design, (8) gives $V_- = 0$ for the $\beta = \text{constant}$ characteristics originating at the load. Finally, because $V_- = 0$ for all characteristic lines incident on the source (whether they originate on the initial conditions or on the load), it follows from (10) that on characteristic lines originating at $z = 0$, V_+ is as shown in Fig. 14.4.5b. We now know V_+ and V_- everywhere.

It follows from (1) and (2) that V and I are as shown in Fig. 14.4.5. Because $V_- = 0$, the voltage and current both take the form of a pulse of temporal duration T and spatial length cT , propagating from source to load with the velocity c .

To express analytically what has been found, we know that at $z = 0$, $V_- = 0$ and in turn from (10) that at $z = 0$,

$$V_+ = \frac{V_g(t)}{\left(\frac{R_g}{Z_o} + 1\right)} \quad (12)$$

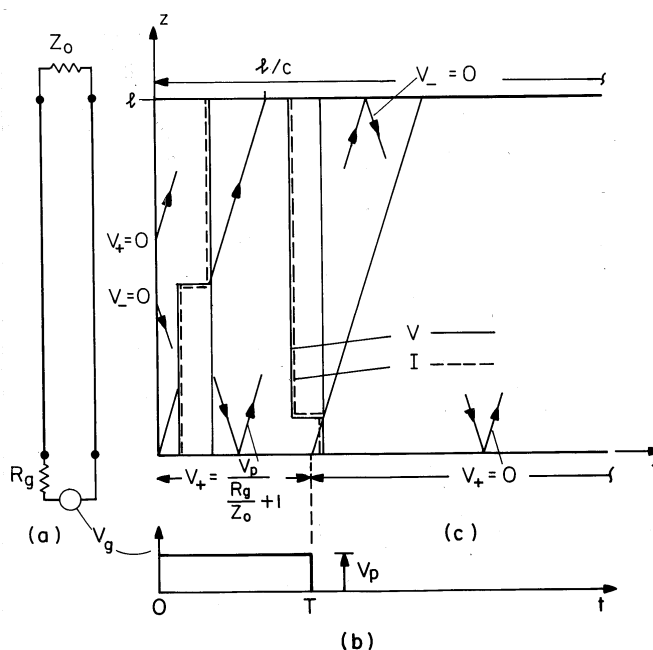


Fig. 14.4.5 (a) Matched line. (b) Wave components in $z-t$ plane. (c) Response in $z-t$ plane.

This is the value of V_+ along any line of constant α originating on the $z = 0$ axis. For example, along the line $\alpha = -ct'$ passing through the $z = 0$ axis when $t = t'$,

$$V_+ = \frac{V_g(t')}{\left(\frac{R_g}{Z_o} + 1\right)} \quad (13)$$

We can express this result in terms of $z-t$ by introducing $\alpha = -ct'$ into (3), solving that expression for t' , and introducing that expression for t' in (13). The result is just what we have already pictured in Fig. 14.4.5.

$$V(z, t) = V_+(\alpha) = \frac{V_g\left(t - \frac{z}{c}\right)}{\left(\frac{R_g}{Z_o} + 1\right)} \quad (14)$$

Regardless of the shape of the voltage pulse, it appears undistorted at some location z but delayed by z/c .

Note that at any location on the matched line, including the terminals of the generator, $V/I = Z_o$. The matched line appears to the generator as a resistance equal to the characteristic impedance of the line.

We have assumed in this example that the initial voltage and current are zero over the length of the line. If there were finite initial conditions, their response with the generator voltage set equal to zero would add to that obtained here because the wave equation is linear and superposition holds. Initial conditions give rise to waves V_+ and V_- propagating in the $+z$ and $-z$ directions, respectively. However, because there are no reflected waves at the load, the effect of the initial conditions could not last longer at the generator than the time l/c required for V_- to reach $z = 0$ from

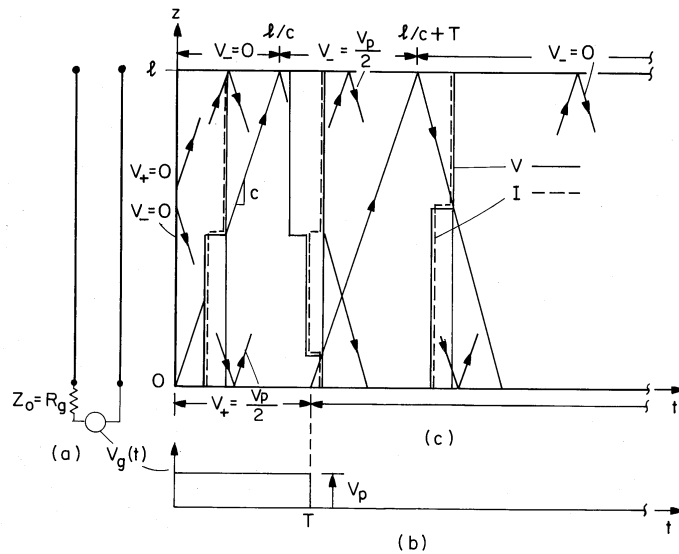


Fig. 14.4.6 (a) Open line. (b) Wave components in $z - t$ plane. (c) Response in $z - t$ plane.

$z = l$. They would not last longer at the load than the time $2l/c$, when any resulting wave reflected from the generator would return to the load.

Open circuit and short circuit terminations result in complete reflection. For the open circuit, $I = 0$ at the termination, and it follows from (2) that $V_+ = V_-$. For a short, $V = 0$, and (1) requires that $V_+ = -V_-$. Note that these limiting relations follow from (8) by making R_L infinite and zero in the respective cases.

In the following example, we see that an open circuit termination can result in a voltage that is momentarily as much as twice that of the generator.

Example 14.4.2. Open Circuit Termination

The transmission line of Fig. 14.4.6 is terminated in an infinite load resistance and driven by a generator modeled as a voltage source in series with a resistance R_g equal to the characteristic impedance Z_o . As in the previous example, the driving voltage is a pulse of time duration T , as shown in Fig. 14.4.6b. When $t = 0$, V and I are zero. In this example, we illustrate the effect of matching the generator resistance to the line and of having complete reflection at the load.

The boundary at $z = l$, (8), requires that

$$V_- = V_+ \tag{15}$$

while that at the generator, (10), is simply

$$V_+ = \frac{V_g}{2} \tag{16}$$

Because the generator is matched, this latter condition establishes V_+ on characteristic lines originating on the $z = 0$ axis without regard for V_- . These are summarized along the t axis in Fig. 14.4.6b.

To establish the values of V_- on characteristic lines originating at the load, we must know values of the incident V_+ . Because I and V are both initially zero, the incident V_+ at the load is zero until $t=l/c$. From (15), V_- is also zero. From $t = l/c$ until $t = l/c + T$, the incident $V_+ = V_p/2$ and V_- on the characteristic lines originating at the open circuit during this time interval follows from (15) as $V_p/2$. Finally, for all greater times, the incident wave is zero at the load and so also is the reflected wave. The values of V_{\pm} for characteristic lines originating on the associated segments of the boundaries and on the $t = 0$ axis are summarized in Fig. 14.4.6c.

With the values of V_{\pm} determined, we now use (1) and (2) to make the picture also shown in Fig. 14.4.6c of the distributions of V and I at progressive instants in time. Because of the matched condition at the generator, the transient is over by the time the pulse has made one round trip. To make the current at the open circuit termination zero, the voltage doubles during that period when both incident and reflected waves exist at the termination.

The configuration of Fig. 14.4.6 was regarded in the previous example as an “open circuit transmission line” driven by a voltage source in series with a resistor. If we had been given the same configuration in Chap. 7, we would have taken it to be a “capacitor” in series with the resistor and the voltage source. The next example puts the EQS approximation in perspective by showing how it represents the dynamics when the resistance R_g is large compared to Z_o . A clue as to what happens when this ratio is large comes from writing it in the form

$$\frac{R_g}{Z_o} = R_g \sqrt{C/L} = \frac{R_g Cl}{l\sqrt{CL}} = \frac{R_g Cl}{(l/c)} \quad (17)$$

Here, $R_g Cl$ is the charging time of the capacitor and l/c is the electromagnetic wave transit time. When this ratio is large, the time for the transient to complete itself is many wave transit times. Thus, as will now be seen, the exponential charging of the capacitor is made up of many small steps associated with the electromagnetic wave passing “to and fro” over the length of the line.

Example 14.4.3. Quasistatic Transient as the Limit of an Electrodynamic Transient

The transmission line shown to the left in Fig. 14.4.7 is open at $z = l$ and driven at $z = 0$ by a step in voltage, $V_g = V_p u_{-1}(t)$. We are especially interested in the response with the series resistance, R_g , very large compared to Z_o . For simplicity, we assume that the initial voltage and current are zero.

The boundary condition imposed at the open termination, where $z = l$, is $I = 0$. From (2),

$$V_+ = V_- \quad (18)$$

while at the source, (10) pertains with $V_g = V_p$ a constant⁵

$$V_+ = V_g + V_- \Gamma_g; \quad V_g \equiv \frac{V_p}{\left(\frac{R_g}{Z_o} + 1\right)} \quad (19)$$

⁵ Be careful to distinguish the constant V_g as defined in this example from the source voltage $V_g(t) = V_p u_{-1}(t)$.

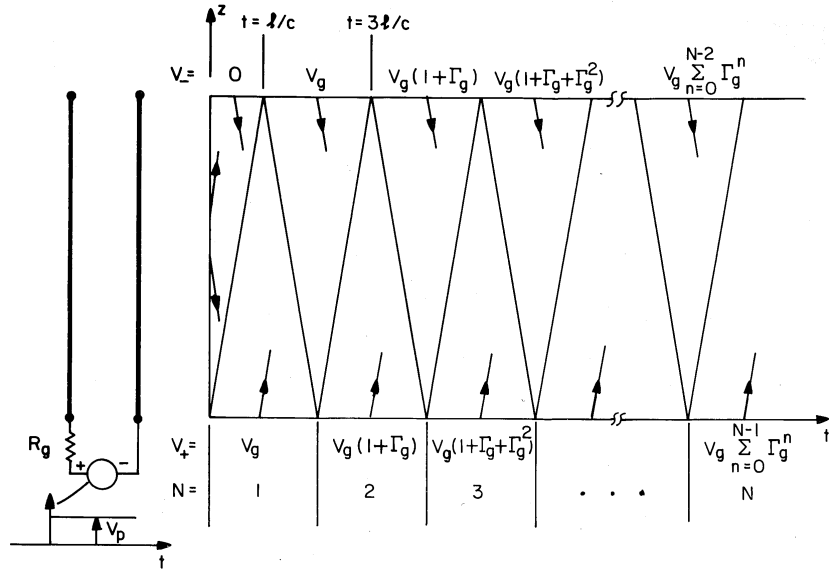


Fig. 14.4.7 Wave components of open line to a step in voltage in series with a high resistance.

with the reflection coefficient of the generator defined as

$$\Gamma_g \equiv \frac{\frac{R_g}{Z_0} - 1}{\frac{R_g}{Z_0} + 1} \quad (20)$$

Starting with characteristic lines originating at $t = 0$, where the initial conditions determine that V_+ and V_- are zero, we can now use these boundary conditions to determine V_- on lines originating at the load and V_+ on lines originating at $z = 0$. These values are shown in Fig. 14.4.7. Thus, V_{\pm} are now known everywhere in the C-shaped region.

The voltage and current now follow from (1) and (2). In particular, consider the response at the generator terminals, where $z = 0$. In Fig. 14.4.7, the t axis has been divided into intervals of duration $2l/c$, the first denoted by $N = 1$, the second by $N = 2$, etc. We have found that the wave components incident on and reflected from the $z = 0$ boundary in the N -th interval are

$$V_- = V_g \sum_{n=0}^{N-2} \Gamma_g^n \quad (21)$$

$$V_+ = V_g \sum_{n=0}^{N-1} \Gamma_g^n \quad (22)$$

It follows from (2) that the current at $z = 0$ during this time interval is

$$I(0, t) = \frac{V_p}{R_g} \frac{1}{1 + \frac{Z_0}{R_g}} \Gamma_g^{N-1}; \quad 2(N-1)\frac{l}{c} < t < 2N\frac{l}{c} \quad (23)$$

In turn, this current can be used to evaluate the terminal voltage.

$$V(0, t) = V_p \left(1 - \frac{\Gamma_g^{N-1}}{1 + \frac{Z_o}{R_g}} \right) \quad (24)$$

With R_g/Z_o very large, it follows from (20) that

$$\Gamma_g \rightarrow \left(1 - 2 \frac{Z_o}{R_g} \right) \quad (25)$$

In this same limit, the term $1 + Z_o/R_g$ in (24) is essentially unity. Thus, (24) becomes approximately

$$V(0, t) \rightarrow V_p \left[1 - \left(1 - \frac{2Z_o}{R_g} \right)^{N-1} \right]; \quad 2(N-1) \frac{l}{c} < t < \frac{2Nl}{c} \quad (26)$$

We suspect that in the limit where the round-trip transit time $2l/c$ is short compared to the charging time $\tau = R_g Cl$, this voltage becomes the step response of the series capacitor and resistor.

$$V(0, t) \rightarrow V_p (1 - e^{-t/\tau}) \quad (27)$$

To see that this is indeed the case, we exploit the fact that

$$\lim_{x \rightarrow 0} (1 - x)^{1/x} = e^{-1} \quad (28)$$

by writing (26) in the form

$$V(0, t) \rightarrow V_p \left\{ 1 - \left[\left(1 - \frac{2Z_o}{R_g} \right)^{1/(2Z_o/R_g)} \right]^{(N-1)(2Z_o/R_g)} \right\} \quad (29)$$

It follows that in the limit where Z_o/R_g is small,

$$V(0, t) \rightarrow V_p \left[1 - e^{-(N-1)(2Z_o/R_g)} \right]; \quad 2(N-1) \frac{l}{c} < t < 2N \frac{l}{c} \quad (30)$$

Remember that N represents the interval of time during which the expression is valid. If we take the time as being that when the interval begins, then

$$2(N-1) \frac{l}{c} \sim t \Rightarrow 2(N-1) = \frac{t}{(l/c)} \quad (31)$$

Substitution of this expression for $2(N-1)$ into (30) and use of (17) then shows that in this high-resistance limit, the voltage does indeed take the exponential form for a charging capacitor, (27), with a charging time $\tau = R_g Cl$. In the example of $V(0, t)$ shown in Fig. 14.4.8, there are 10 round-trip transit times in one charging time, $R_g Cl = 20l/c$.

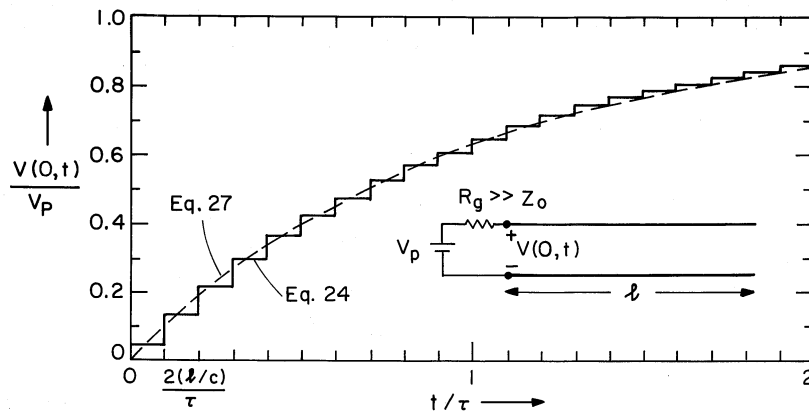


Fig. 14.4.8 Response of open circuit transmission line to step in voltage in series with a high resistance. The smooth curve is predicted by the EQS model.

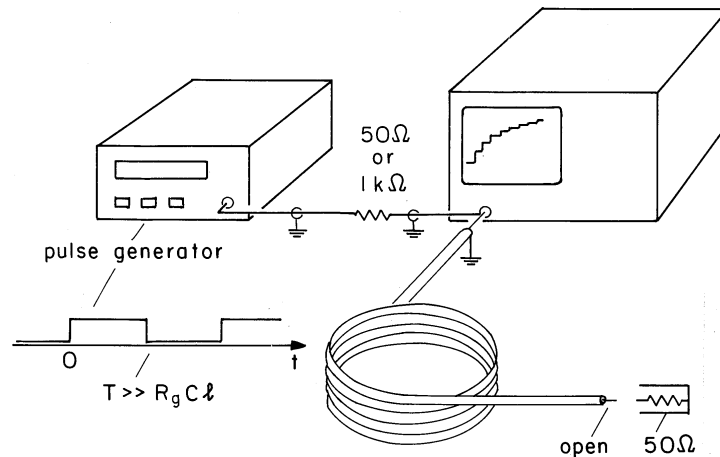


Fig. 14.4.9 Oscilloscope displays voltage at terminals of line under conditions of Examples 14.4.1-3.

The following demonstration is typical of a variety of demonstrations that are easily carried out using a good oscilloscope and a stretch of transmission line.

Demonstration 14.4.1. Transmission Line Matching, Reflection, and Quasi-static Charging

The apparatus shown in Fig. 14.4.9 is all that is required to demonstrate the phenomena described in the examples. In a typical experiment, a 10 m length of cable is used, in which case the wave transit time is about $0.05 \mu s$. Thus, to resolve the transient, the oscilloscope must have a frequency response that extends to 100 MHz.

To achieve matching of the generator, as called for in Example 14.4.2, $R_g = Z_o$. Typically, for a coaxial cable, this is 50Ω .

To see the charging transient of Example 14.4.3 with 10 round trip transit times in the capacitive charging time, it follows from (17) that we should make $R_g/Z_o = 20$. Thus, for a coaxial cable having $Z_o = 50\Omega$, $R_g = 1k\Omega$.

14.5 TRANSMISSION LINES IN THE SINUSOIDAL STEADY STATE

The method used in Sec. 14.4 is equally applicable to finding the response to a sinusoidal excitation of an ideal transmission line. Rather than exciting the line by a voltage step or a voltage pulse, as in the examples of Sec. 14.4, the source may produce a sinusoidal excitation. In that case, there is a part of the response that is in the sinusoidal steady state and a part that accounts for the initial conditions and the transient associated with turning on the source. Provided that the boundary conditions are (like the transmission line equations) linear, we can express the response as a superposition of these two parts.

$$V(z, t) = V_s(z, t) + V_t(z, t) \quad (1)$$

Here, V_s is the sinusoidal steady state response, determined without regard for the initial conditions but satisfying the boundary conditions. Added to this to make the total solution satisfy the initial conditions is V_t . This transient solution is defined to satisfy the boundary conditions with the drive equal to zero and to make the total solution satisfy the initial conditions. If we were interested in it, this transient solution could be found using the methods of the previous section. In an actual physical situation, this part of the solution is usually dissipated in the resistances of the terminations and the line itself. Then the sinusoidal steady state prevails. In this and the next section, we focus on this part of the solution.

With the understanding that the boundary conditions, like those describing the transmission line, are linear differential equations with constant coefficients, the response will be sinusoidal and at the same frequency, ω , as the drive. Thus, we assume at the outset that

$$V = \text{Re } \hat{V}(z)e^{j\omega t}; \quad I = \text{Re } \hat{I}(z)e^{j\omega t} \quad (2)$$

Substitution of these expressions into the transmission line equations, (14.1.4)–(14.1.5), shows that the z dependence is governed by the ordinary differential equations

$$\boxed{\frac{d\hat{I}}{dz} = -j\omega C\hat{V}} \quad (3)$$

$$\boxed{\frac{d\hat{V}}{dz} = -j\omega L\hat{I}} \quad (4)$$

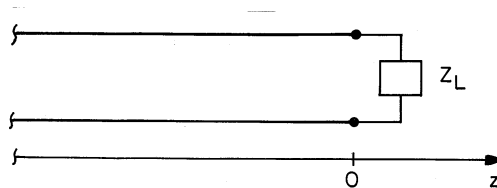


Fig. 14.5.1 Termination at $z = 0$ in load impedance.

Again because of the constant coefficients, these linear equations have two solutions, each having the form $\exp(-jkz)$. Substitution shows that

$$\hat{V} = \hat{V}_+ e^{-j\beta z} + \hat{V}_- e^{j\beta z} \quad (5)$$

where $\beta \equiv \omega\sqrt{LC}$. In terms of the same two arbitrary complex coefficients, it also follows from substitution of this expression into (14.1.5) that

$$\hat{I} = \frac{1}{Z_o} (\hat{V}_+ e^{-j\beta z} - \hat{V}_- e^{j\beta z}) \quad (6)$$

where $Z_o = \sqrt{L/C}$.

What we have found are solutions having the same traveling wave forms as identified in Sec. 14.3, (14.3.9)–(14.3.10). This can be seen by using (2) to recover the time dependence and writing these two expressions as

$$V = \text{Re} \left[\hat{V}_+ e^{-j\beta(z - \frac{\omega}{\beta}t)} + \hat{V}_- e^{j\beta(z + \frac{\omega}{\beta}t)} \right] \quad (7)$$

$$I = \text{Re} \frac{1}{Z_o} \left[\hat{V}_+ e^{-j\beta(z - \frac{\omega}{\beta}t)} - \hat{V}_- e^{j\beta(z + \frac{\omega}{\beta}t)} \right] \quad (8)$$

The velocity of the waves is $\pm\omega/\beta = 1/\sqrt{LC}$. Because the coefficients \hat{V}_\pm are complex, they represent both the amplitude and phase of these traveling waves. Thus, the solutions could be sinusoids, cosinusoids, or any combination of these having the given arguments. In working with standing waves in Sec. 13.2, we demonstrated how the coefficients could be adjusted to satisfy simple boundary conditions. Here we introduce a point of view that is convenient in dealing with complicated terminations.

Transmission Line Impedance. The transmission line shown in Fig. 14.5.1 is terminated in a load impedance Z_L . By definition, Z_L is the complex number

$$\frac{\hat{V}(0)}{\hat{I}(0)} = Z_L \quad (9)$$

In general, it could represent any linear system composed of resistors, inductors, and capacitors. The complex amplitudes \hat{V}_\pm are determined by this and another boundary condition. This second condition represents the termination of the line somewhere to the left in Fig. 14.5.1.

At any location on the line, the impedance is found by taking the ratio of (5) and (6).

$$\boxed{Z(z) \equiv \frac{\hat{V}(z)}{\hat{I}(z)} = Z_o \frac{1 + \Gamma_L e^{2j\beta z}}{1 - \Gamma_L e^{2j\beta z}}} \quad (10)$$

Here, Γ_L is the *reflection coefficient* of the load.

$$\boxed{\Gamma_L \equiv \frac{\hat{V}_-}{\hat{V}_+}} \quad (11)$$

Thus, Γ_L is simply the ratio of the complex amplitudes of the traveling wave components.

At the location $z = 0$, where the line is connected to the load and (9) applies, this expression becomes

$$\boxed{\frac{Z_L}{Z_o} = \frac{1 + \Gamma_L}{1 - \Gamma_L}} \quad (12)$$

The boundary condition, expressed by (12), is sufficient to determine the reflection coefficient. That is, from (12) it follows that

$$\Gamma_L = \frac{(Z_L/Z_o - 1)}{(Z_L/Z_o + 1)} \quad (13)$$

Given the load impedance, Γ_L follows from this expression. The line impedance at a location z to the left then follows from the use of this expression to evaluate (10).

The following examples lead to important implications of (11) while indicating the usefulness of the impedance point of view.

Example 14.5.1. Impedance Matching

Given an incident wave V_+ , how can we eliminate the reflected wave represented by V_- ? By definition, there is no reflected wave if the reflection coefficient, (11), is zero. It follows from (13) that

$$\Gamma_L = 0 \Rightarrow Z_L = Z_o \quad (14)$$

Note that Z_o is real, which means that the matched load is equivalent to a resistance, $R_L = Z_o$. Thus, our finding is consistent with that of Sec. 14.4, where we found that

such a termination would eliminate the reflected wave, sinusoidal steady state or not.

It follows from (10) that the line has the same impedance, Z_o , at any location z , when terminated in its characteristic impedance. Because $V_- = 0$, it follows from (7) that the voltage takes the form

$$V = \text{Re } \hat{V}_+ e^{j(\omega t - \beta z)} \quad (15)$$

The voltage has the distribution in space and time of a sinusoid traveling in the z direction with the velocity $1/\sqrt{LC}$. At any given location, the voltage is sinusoidal in time at the (angular) frequency ω . The amplitude is the same, regardless of z .⁶

The previous example illustrated that at any location, a transmission line terminated in a resistance equal to its characteristic impedance has an impedance which is also resistive and equal to Z_o . The next example illustrates what happens in the opposite extreme, where the termination dissipates no energy and the response is a pure standing wave rather than the pure traveling wave of the matched line.

Example 14.5.2. Short Circuit Impedance and Standing Waves

With a short circuit at $z = 0$, (5) makes it clear that $V_- = -V_+$. Thus, the reflection coefficient defined by (11) is $\Gamma_L = -1$. We come to the same conclusion from the evaluation of (13).

$$Z_L = 0 \Rightarrow \Gamma_L = -1 \quad (16)$$

The impedance at some location z then follows from (10) as

$$\frac{Z(-l)}{Z_o} \equiv j \frac{X}{Z_o} = j \tan \beta l \quad (17)$$

In view of the definition of β ,

$$\beta l = \frac{\omega l}{c} = 2\pi \frac{l}{\lambda} \quad (18)$$

and so we can think of βl as being proportional either to the frequency or to the length of the line measured in wavelengths λ . The impedance of the line is a reactance X having the dependence on either of these quantities shown in Fig. 14.5.2.

At low frequencies (or for a length that is short compared to a quarter-wavelength), X is positive and proportional to ω . As should be expected from either Chap. 8 or Example 13.1.1, the reactance is that of an inductor.

$$\beta l \ll 1 \Rightarrow X \rightarrow (\beta l) \sqrt{L/C} = \omega L l \quad (19)$$

As the frequency is raised to the point where the line is a quarter-wavelength long, the impedance is infinite. A shorted quarter-wavelength line has the impedance of an open circuit! As the frequency is raised still further, the reactance becomes capacitive, decreasing with increasing frequency until the half-wavelength line exhibits

⁶ By contrast with Demonstration 13.1.1, where the light emitted by the fluorescent tube indicated that the electric field peaked at some locations and nulled at others, the distribution of light for a matched line would be “flat.”

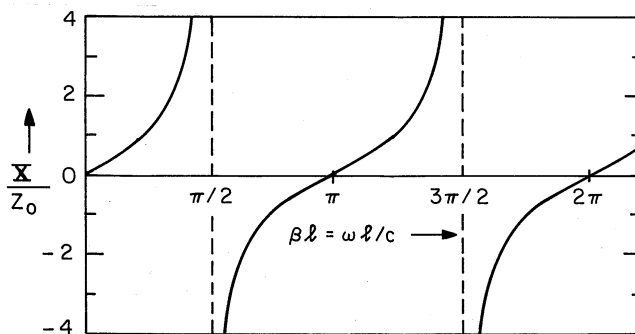


Fig. 14.5.2 Reactance as a function of normalized frequency for a shorted line.

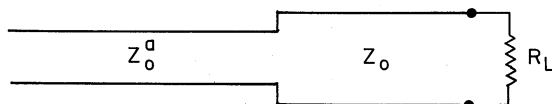


Fig. 14.5.3 A quarter-wave matching section.

the impedance of the termination, a short. That the impedance repeats itself as the line is increased in length by a half-wavelength is evident from Fig. 14.5.2.

We consider next an example that illustrates one of many methods for matching a load resistance R_L to a line having a characteristic impedance not equal to R_L .

Example 14.5.3. Quarter-Wave Matching Section

A quarter-wavelength line, as shown in Fig. 14.5.3, has the useful property of converting a normalized load impedance Z_L/Z_0 to a normalized impedance that is the reciprocal of that impedance, Z_0/Z_L . To see this, we evaluate the impedance, (10), a quarter-wavelength from the load, where $\beta z = -\pi/2$, and then use (12).

$$Z(\beta z = -\frac{\pi}{2}) = \frac{Z_0^2}{Z_L} \quad (20)$$

Thus, if we wanted to match a line having the characteristic impedance Z_0^a to a load resistance $Z_L = R_L$, we could interpose a quarter-wavelength section of line having as its characteristic impedance a Z_0 that is the geometric mean of the load resistance and the characteristic impedance of the line to be matched.

$$Z_0 = \sqrt{Z_0^a R_L} \quad (21)$$

The idea of using quarter-wavelength sections to achieve matching will be continued in the next example.

The transmission line model is equally well applicable to electromagnetic plane waves. The equivalence was pointed out in Sec. 14.1. When these waves are optical, the permeability of common materials remains μ_0 , and the polarizability is

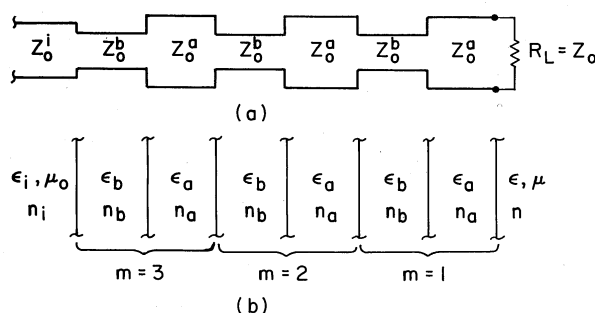


Fig. 14.5.4 (a) Cascaded quarter-wave transmission line sections. (b) Optical coating represented by (a).

described by the *index of refraction*, n , defined such that

$$\mathbf{D} = n^2 \epsilon_o \mathbf{E} \tag{22}$$

Thus, $n^2 \epsilon_o$ takes the place of the dielectric constant, ϵ . The appropriate value of $n^2 \epsilon_o$ is likely to be very different from the value of ϵ used for the same material at low frequencies.⁷

The following example illustrates the application of the transmission line viewpoint to an optical problem.

Example 14.5.4. Quarter-Wave Cascades for Reduction of Reflection

When *one* quarter-wavelength line is used to transform from one specified impedance to another, it is necessary to specify the characteristic impedance of the quarter-wave section. In optics, where it is desirable to minimize reflections that result from the passage of light from one transparent medium to another, it is necessary to specify the index of refraction of the quarter wave section. Given other constraints on the materials, this often is not possible. In this example, we see how the use of multiple layers gives some flexibility in the choice of materials.

The matching section of Fig. 14.5.4a consists of m pairs of quarter-wave sections of transmission line, respectively, having characteristic impedances Z_o^a and Z_o^b . This represents equally well the cascaded pairs of quarter wave layers of dielectric shown in Fig. 14.5.4b, interposed between materials of dielectric constants ϵ and ϵ_i . Alternatively, these layers are represented by their indices of refraction, n_a and n_b , interposed between materials having indices n_i and n .

First, we picture the matching problem in terms of the transmission line. The load resistance R_L represents the material to the right of the cascade. This region is pictured as an infinite transmission line having characteristic impedance Z_o . Thus, it presents a load to the cascade of resistance $R_L = Z_o$. To determine the impedance at the other side of the cascade, we make repeated use of the impedance transformation for a quarter-wave section, (20). To begin with, the impedance at the terminals of the first quarter-wave section is

$$Z = \frac{(Z_o^a)^2}{Z_o} \tag{23}$$

⁷ With fields described in the frequency domain, ϵ , and hence n^2 , are in general complex functions of frequency, as in Sec. 11.5.

With this taken as the load resistance in (20), the impedance at the terminals of the second section is

$$Z = \left(\frac{Z_o^b}{Z_o^a} \right)^2 Z_o \quad (24)$$

This can now be regarded as the impedance transformation for the pair of quarter-wave sections. If we now make repeated use of (24) to represent the impedance transformation for the quarter-wave sections taken in pairs, we find that the impedance at the terminals of m pairs is

$$Z = \left(\frac{Z_o^b}{Z_o^a} \right)^{2m} Z_o \quad (25)$$

Now, to apply this result to the optics configuration, we identify (14.1.9)

$$\begin{aligned} R_L &\rightarrow \sqrt{\mu_o/\epsilon} \equiv \zeta_L = \frac{\zeta_o}{n}; \\ Z_o^a &= \sqrt{\mu_o/\epsilon_a} \equiv \zeta_a = \frac{\zeta_o}{n_a}; \\ Z_o^b &= \sqrt{\mu_o/\epsilon_b} \equiv \zeta_b = \frac{\zeta_o}{n_b} \end{aligned} \quad (26)$$

and have from (25) for the intrinsic impedance of the cascade

$$\zeta = \zeta_L \left(\frac{\zeta_b}{\zeta_a} \right)^{2m} \quad (27)$$

In terms of the indices of refraction,

$$\frac{n}{n_i} = \left(\frac{n_a}{n_b} \right)^{2m} \quad (28)$$

If this condition on the optical properties and number of the layer pairs is fulfilled, the wave can propagate through the interface between regions of indices n_i and n without reflection. Given materials having n_a/n_b less than n/n_i , it is possible to pick the number of layer pairs, m , to satisfy the condition (at least approximately).

Coatings are commonly used on lenses to prevent reflection. In such applications, the waves processed by the lens generally have a spectrum of frequencies. Thus, optimization of the matching coatings is more complex than pictured here, where it has been assumed that the light is at a single frequency (is monochromatic).

It has been assumed here that the electromagnetic wave has normal incidence at the dielectric interface. Waves arriving at the interface at an angle can also be pictured in terms of the transmission line. In practical applications, the design of lens coatings to prevent reflection over a range of angles of incidence is a further complication.⁸

⁸ H. A. Haus, *Waves and Fields in Optoelectronics*, Prentice-Hall, Inc., Englewood Cliffs, N.J. (1984), pp. 43-46.

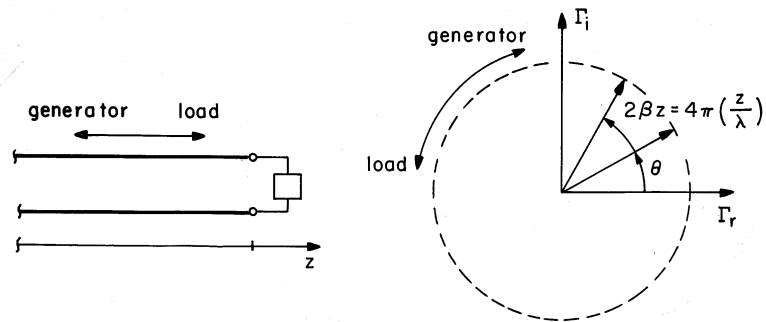


Fig. 14.6.1 (a) Transmission line conventions. (b) Reflection coefficient dependence on z in the complex Γ plane.

14.6 REFLECTION COEFFICIENT REPRESENTATION OF TRANSMISSION LINES

In Sec. 14.5, we found that a quarter-wavelength of transmission line turned a short circuit into an open circuit. Indeed, with an appropriate length (or driven at an appropriate frequency), the shorted line could have an inductive or a capacitive reactance. In general, the impedance observed at the terminals of a transmission line has a more complicated dependence on the termination.

Typical microwave measurements are made with a length of transmission line between the observation point and the terminals of the device under study, whether that be an antenna or a transistor. In this section, the objective is a way of visualizing the relation between the impedance at the “generator” terminals and the impedance of the “load.” We will find that a representation of the variables in the reflection coefficient plane is valuable both conceptually and practically.

At a location z , the impedance of the transmission line shown in Fig. 14.6.1a is (14.5.10)

$$\frac{Z(z)}{Z_o} = \frac{1 + \Gamma(z)}{1 - \Gamma(z)} \tag{1}$$

where the reflection coefficient at the location z is defined as the complex function

$$\Gamma(z) = \frac{\hat{V}_-}{\hat{V}_+} e^{j2\beta z} \tag{2}$$

At the load position, where $z = 0$, the reflection coefficient is equal to Γ_L as defined by (14.5.11).

Like the impedance, the reflection coefficient is a function of z . Unlike the impedance, Γ has an easily pictured z dependence. Regardless of z , the magnitude of Γ is the same. Thus, as pictured in the complex Γ plane of Fig. 14.6.1b, it is a complex vector of magnitude $|\hat{V}_-/\hat{V}_+|$ and angle $\theta + 2\beta z$, where θ is the angle at

the position $z = 0$. With z defined as increasing from the generator to the load, the dependence of the reflection coefficient on z is as summarized in the figure. As we move from the generator toward the load, z increases and hence Γ rotates in the counterclockwise direction.

In summary, once the complex number Γ is established at one location z , its variation as we move toward the load or toward the generator can be pictured as a rotation at constant magnitude in the counterclockwise or clockwise directions, respectively. Typically, Γ is established at the location of the load, where the impedance, Z_L , is known. Then Γ at any location z follows from (1) solved for Γ .

$$\Gamma = \frac{\left(\frac{Z}{Z_o} - 1\right)}{\left(\frac{Z}{Z_o} + 1\right)} \quad (3)$$

With the magnitude and phase of Γ established at the load, the reflection coefficient can be found at another location by a simple rotation through an angle $4\pi(z/\lambda)$, as shown in Fig. 14.6.1b. The impedance at this second location would then follow from evaluation of (1).

Smith Chart. We save ourselves the trouble of evaluating (1) or (3), either to establish Γ at the load or to infer the impedance implied by Γ at some other location, by mapping Z/Z_o in the Γ plane of Fig. 14.6.1b. To this end, we define the normalized impedance as having a resistive part r and a reactive part x

$$\frac{Z}{Z_o} = r + jx \quad (4)$$

and plot the contours of constant r and of constant x in the Γ plane. This makes it possible to see directly what Z is implied by each value of Γ . Effectively, such a mapping provides a graphical solution of (1). The next few steps summarize how this mapping of the contours of constant r and x in the $\Gamma_r - \Gamma_i$ plane can be made with ruler and compass.

First, (1) is written using (4) on the left and $\Gamma = \Gamma_r + j\Gamma_i$ on the right. The real and imaginary parts of this equation must be equal, so it follows that

$$r = \frac{(1 - \Gamma_r^2 - \Gamma_i^2)}{(1 - \Gamma_r)^2 + \Gamma_i^2} \quad (5)$$

$$x = \frac{2\Gamma_i}{(1 - \Gamma_r)^2 + \Gamma_i^2} \quad (6)$$

These expressions are quadratic in Γ_r and Γ_i . By completing the squares, they can be written as

$$\left(\Gamma_r - \frac{r}{r+1}\right)^2 + \Gamma_i^2 = \left(\frac{1}{1+r}\right)^2 \quad (7)$$

$$(\Gamma_r - 1)^2 + \left(\Gamma_i - \frac{1}{x}\right)^2 = \left(\frac{1}{x}\right)^2 \quad (8)$$

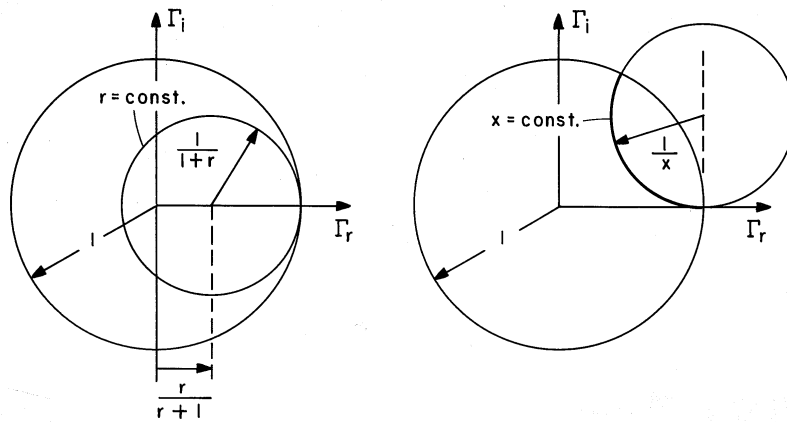


Fig. 14.6.2 (a) Circle of constant normalized resistance, r , in Γ plane. (b) Circle of constant normalized reactance, x , in Γ plane.

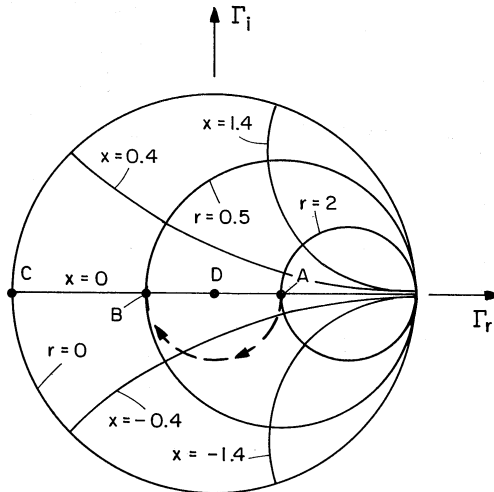


Fig. 14.6.3 Smith chart.

Thus, the contours of constant normalized resistance, r , and of constant normalized reactance, x , are the circles shown in Figs. 14.6.2a–14.6.2b.

Putting these contours together gives the lines of constant r and x in the complex Γ plane shown in Fig. 14.6.3. This is called a *Smith chart*.

Illustration. Impedance with Simple Terminations

How do we interpret the examples of Sec. 14.5 in terms of the Smith chart?

- **Quarter-wave Section.** In Example 14.5.3 we found that a normalized resistive load r_L was transformed into its reciprocal by a quarter-wave line. Suppose that $r_L = 2$ (the load resistance is $2Z_o$) and $x = 0$. Then, the load is

at A in Fig. 14.6.3. A quarter-wavelength toward the generator is a rotation of 180 degrees in a clockwise direction, with Γ following the trajectory from $A \rightarrow B$ in Fig. 14.6.3. Note that the impedance at B is indeed the reciprocal of that at A , $r = 0.5, x = 0$.

- **Impedance of Short Circuit Line.** Consider next the shorted line of Example 14.5.2. The load resistance r_L is 0, and reactance x_L is 0 as well, so we begin at the point C in Fig. 14.6.3. Now, we can trace out the impedance as we move away from the short toward the generator by rotating along the trajectory of unit radius in the clockwise direction. Note that all along this trajectory, $r = 0$. The normalized reactance then traces out the values given in Fig. 14.5.2, first taking on positive (inductive) values until it becomes infinite at $\lambda/4$ (rotation of 180 degrees), and then negative (capacitive) values until it returns to C , when the line has a length of $\lambda/2$.
- **Matched Line.** For the matched load of Example 14.5.1, we start out with $r_L = 1$ and $x_L = 0$. This is point D at the origin in Fig. 14.6.3. Thus, the trajectory of Γ is a circle of zero radius, and the impedance remains $r_L = 1$ over the length of the line.

While taking measurements on a transmission line terminated in a particular device, the Smith chart is often used to have an immediate picture of the impedance at the terminals. Even though the chart could be replaced by a programmable calculator, the overview provided by the Smith chart is important. Not only does it provide insight concerning the impedance, it can be used to picture the spatial evolution of the voltage and current, as we now see.

Standing Wave Ratio. Once the reflection coefficient has been established, the voltage and current distributions are determined (to within a factor determined by the source). That is, in terms of Γ , (14.5.5) becomes

$$\hat{V} = \hat{V}_+ e^{-j\beta z} [1 + \Gamma(z)] \quad (9)$$

The exponential factor has an amplitude that is independent of z . Thus, $[1 + \Gamma(z)]$ represents the z dependence of the voltage amplitude. This complex quantity can be pictured in the Γ plane as shown in Fig. 14.6.4a. Remember, as we move from load to generator, Γ rotates in the clockwise direction. As it does so, $1 + \Gamma$ varies between a maximum value of $1 + |\Gamma|$ and a minimum value of $1 - |\Gamma|$. According to (9), we can now picture the spatial distribution of the voltage amplitude. Convenient for describing this distribution is the *voltage standing wave ratio* (VSWR), defined as the ratio of the maximum voltage amplitude to the minimum voltage amplitude. From Fig. 14.6.4a, we can see that this ratio is

$$\text{VSWR} = \frac{(1 + \Gamma)_{\max}}{(1 + \Gamma)_{\min}} = \frac{1 + |\Gamma|}{1 - |\Gamma|} \quad (10)$$

The distribution of voltage amplitude is shown for several VSWR's in Fig. 14.6.4b. We have already seen such distributions in two extremes. With the short

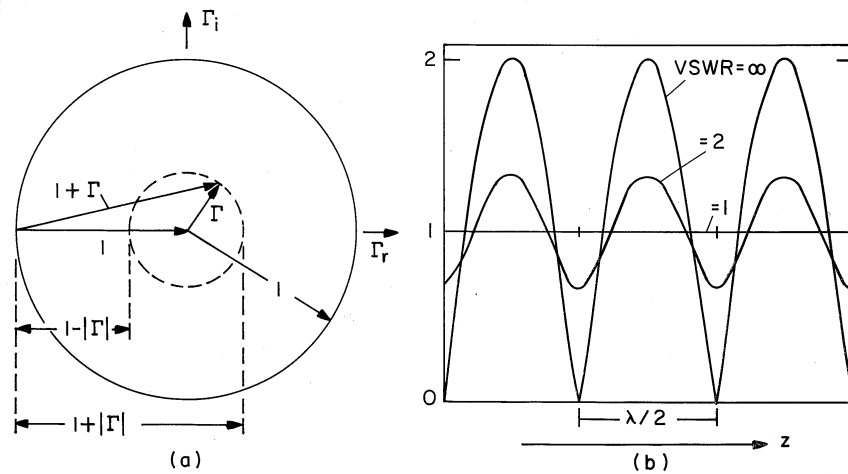


Fig. 14.6.4 (a) Normalized line voltage $1 + \Gamma$. (b) Distribution of voltage amplitude for three VSWR's.

circuit or open circuit terminations considered in Sec. 13.1, the reflection coefficient was on the unit circle and the VSWR was infinite. Indeed, the infinite VSWR envelope of Fig. 14.6.4b is that of a standing wave, with nulls every half-wavelength. The opposite extreme is also familiar. Here, the line is matched and the reflection coefficient is on a circle of zero radius. Thus, the VSWR is unity and the distribution of voltage amplitude is uniform.

Measurement of the VSWR and the location of a voltage null provides the information needed to determine a line termination. This follows by first using (10) to evaluate the magnitude of the reflection coefficient from the measured VSWR.

$$|\Gamma| = \frac{\text{VSWR} - 1}{\text{VSWR} + 1} \tag{11}$$

Thus, the radius of the circle representing the voltage distribution on the line has been determined. Second, a determination of the position of a null is tantamount to locating (to within a half-wavelength) the position on the line where Γ passes through the negative real axis. The distance from this point to the load, in wavelengths, then determines where the load is located on this circle. The corresponding impedance is that of the load.

Demonstration 14.6.1. VSWR and Load Impedance

In the slotted line shown in Fig. 14.6.5, a movable probe with its attached detector provides a measure of the line voltage as a function of z . The distance between the load and the voltage probe can be measured directly. By using a frequency of 3 GHz and an air-insulated cable (having a permittivity that is essentially that of free space, so that the wave velocity is 3×10^8 m/s), the wavelength is conveniently 10 cm.

The characteristic impedance of the coaxial cable is 50Ω , so with terminations of 50Ω , 100Ω , and a short, the observed distribution of voltage is as shown in Fig. 14.6.4b for VSWR's of 1, 2, and ∞ . (To plot data points on these curves, the

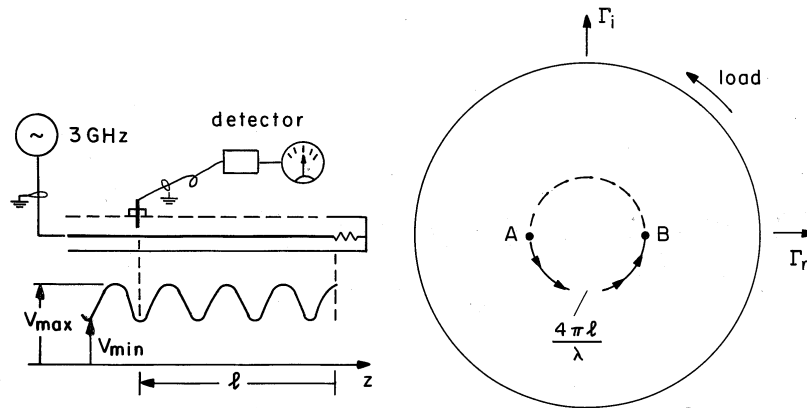


Fig. 14.6.5 Demonstration of distribution of voltage magnitude as function of VSWR.

measured values should be normalized to match the peak voltage of the appropriate distribution.)

Figure 14.6.5 illustrates how a measurement of the VSWR and position of a null can be used to infer the termination. Addition of a half-wavelength to l means an additional revolution in the Γ plane, so which null is used to define the distance l makes no difference. The trajectory drawn in the illustration is for the 100 Ω termination.

Admittance in the Reflection Coefficient Plane. Commonly, transmission lines are interconnected in parallel. It is then convenient to work with the admittance rather than the impedance. The Smith chart describes equally well the evolution of the admittance with z .

With $Y_o = 1/Z_o$ defined as the characteristic admittance, it follows from (1) that

$$\frac{Y}{Y_o} = \frac{1 - \Gamma}{1 + \Gamma} \quad (12)$$

If $\Gamma \rightarrow -\Gamma$, this expression becomes identical to that relating the normalized impedance to Γ , (1). Thus, the contours of constant normalized conductance, g , and normalized susceptance, y ,

$$\frac{Y}{Y_o} \equiv g + jy \quad (13)$$

are those of the normalized impedance, r and x , rotated by 180 degrees. Rotate by 180 degrees the impedance form of the Smith chart and the admittance form is obtained! The contours of r and x , respectively, become those of g and y .⁹

⁹ Usually, Γ is not explicitly evaluated. Rather, the admittance is given at one point on the Γ circle (and hence on the chart) and determined (by a rotation through the appropriate angle on the chart) at another point. Thus, for most applications, the chart need not even be rotated. However, if Γ is to be evaluated directly from the admittance, it should be remembered that the coordinates are actually $-\Gamma_r$ and $-\Gamma_i$.

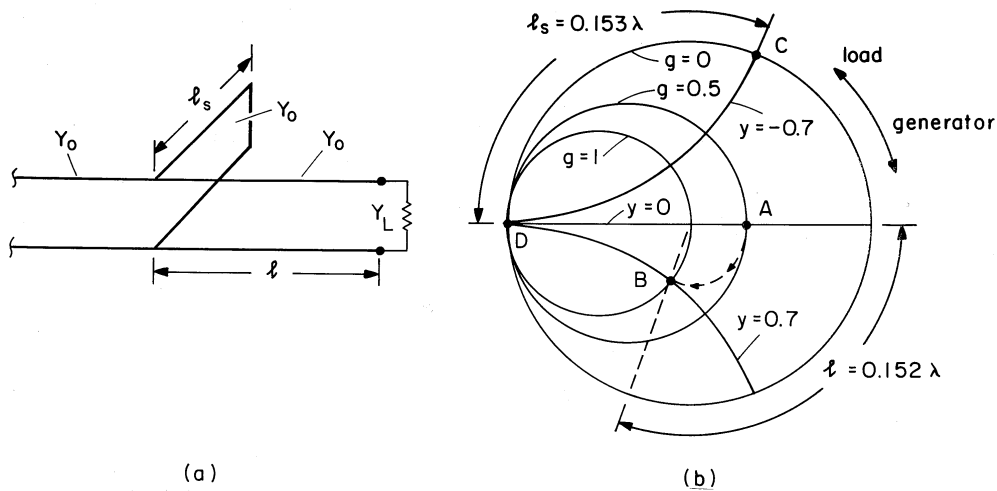


Fig. 14.6.6 (a) Single stub matching. (b) Admittance Smith chart.

The admittance form of the Smith chart is used in the following example.

Example 14.6.1. Single Stub Matching

In Fig. 14.6.6a, the load admittance Y_L is to be matched to a transmission line having characteristic admittance Y_0 by means of a “stub” consisting of a shorted section of line having the same characteristic admittance Y_0 . Variables that can be used to accomplish the matching are the distance l from the load to the stub and the length l_s of the stub.

Matching is accomplished in two steps. First, the length l is adjusted so that the real part of the admittance at the position where the stub is attached is equal to Y_0 . Then the length of the shorted stub is adjusted so that its susceptance cancels that of the line. Here, we see the reason for using the admittance form of the Smith chart, shown in Fig. 14.6.6b. The stub and the line are connected in parallel so that their admittances add.

The two steps are pictured in Fig. 14.6.6b for the case where the normalized load admittance is $g + jy = 0.5$, at A on the chart. The real part of the admittance becomes equal to the characteristic admittance on the circle $g = 1$; we adjust the length l so that the stub is connected at B , where the $|\Gamma|$ constant curve intersects the $g = 1$ circle. In the particular example shown, this length is $l = 0.152\lambda$. From the chart, one reads off a positive susceptance at this point of about $y = 0.7$. We can determine the stub length l_s that gives the negative of this susceptance by again using the chart. The desired admittance of the stub is at C , where $g = 0$ and $y = -0.7$. In the case of the stub, the “load” is the short, where the admittance is infinite, at D on the chart. Following the $|\Gamma| = 1$ circle in the clockwise direction (from the “load” toward the “generator”) from the short at D to the desired admittance at C then gives the length of the stub. For the example, $l_s = 0.153\lambda$.

To the left of the point where the stub is attached, the line should have a unity VSWR. The following demonstrates this concept.

Demonstration 14.6.2. Single Stub Matching

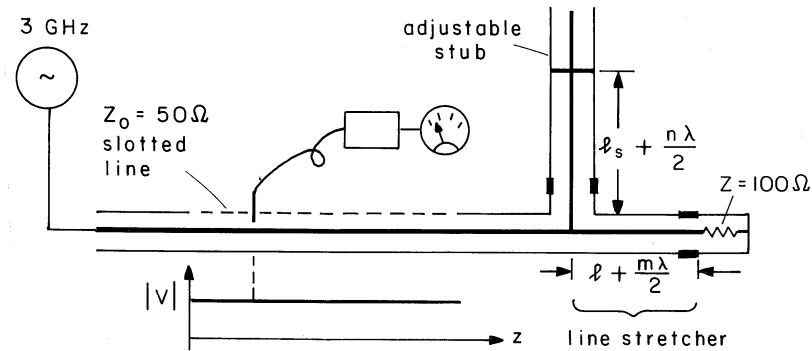


Fig. 14.6.7 Single stub matching demonstration.

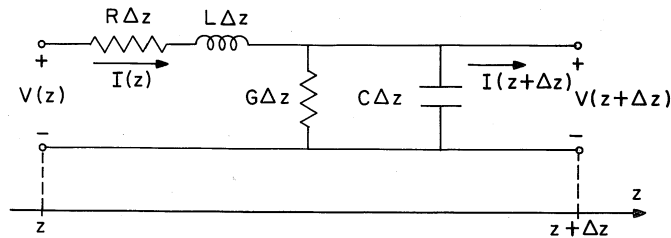


Fig. 14.7.1 Incremental section of lossy distributed line.

In Fig. 14.6.7, the previous demonstration has been terminated with an adjustable length of line (a line stretcher) and a stub. The slotted line makes it possible to see the effect on the VSWR of matching the line. With a load of $Z = 100\Omega$ and the stub and line stretcher adjusted to the values found in the previous example, the voltage amplitude is found to be independent of the position of the probe in the slotted line. Of course, we can add a half-wavelength to either l or l_s and obtain the same condition.

14.7 DISTRIBUTED PARAMETER EQUIVALENTS AND MODELS WITH DISSIPATION

The distributed parameter transmission line of Sec. 14.1 is now generalized to include certain types of dissipation by using the incremental circuit shown in Fig. 14.7.1. The capacitance per unit length C is shunted by a conductance per unit length G and in series with the inductance per unit length L is the resistance per unit length R .

If the line really were made up of so many lumped parameter elements that it could be described by continuum equations, G would be the conductance per unit length of the lossy capacitors (Sec. 7.9) and R would be the resistance per unit length of the inductors. More often, G and R (like L and C) are either equivalent to or a model of a physical system. Examples are discussed in the next two sections.

The steps leading to the generalized transmission line equations are suggested by Eqs. 14.1.1 through 14.1.5. In requiring that the currents at the terminal on the right sum to zero, there is now an additional current through the shunt conductance. In the limit where $\Delta z \rightarrow 0$,

$$\boxed{\frac{\partial I}{\partial z} = -C \frac{\partial V}{\partial t} - GV} \quad (1)$$

Similarly, in summing the voltages around the loop, there is now a voltage drop across the series resistance. Again, in the limit $\Delta z \rightarrow 0$,

$$\boxed{\frac{\partial V}{\partial z} = -L \frac{\partial I}{\partial t} - RI} \quad (2)$$

As should be expected, with the introduction of dissipation represented by G and R , $V(z, t)$ and $I(z, t)$ no longer take the form of waves propagating without distortion. That is, substitution shows that solutions no longer take the form of (14.4.1)–(14.4.3). As a result, we would have to work considerably harder than in Secs. 14.3–14.4 to describe transients on lossy transmission lines. However, although somewhat more involved than before, the sinusoidal steady state response follows from the approach illustrated in Secs. 14.5–14.6.

With the objective of describing the sinusoidal steady state, complex amplitude representations of V and I (14.5.2) are substituted into (1) and (2) to give

$$\frac{d\hat{I}}{dz} = -(j\omega C + G)\hat{V} \quad (3)$$

$$\frac{d\hat{V}}{dz} = -(j\omega L + R)\hat{I} \quad (4)$$

To obtain an expression for the voltage alone, (3) is substituted into the derivative of (4).

$$\frac{d^2\hat{V}}{dz^2} - (j\omega L + R)(j\omega C + G)\hat{V} = 0 \quad (5)$$

With the voltage found from this equation, the current follows from (4).

$$\hat{I} = \frac{-1}{R + j\omega L} \frac{d\hat{V}}{dz} \quad (6)$$

Albeit complex, the coefficient in (5) is constant, so it is again appropriate to look for exponential solutions. Using the convention established in Sec. 14.5, we look for solutions $\exp(-jkz)$. Substitution into (5) then shows that

$$k^2 = -(j\omega L + R)(j\omega C + G) \quad (7)$$

So as to be clear in distinguishing the two roots of this dispersion equation, we *define* β as having a positive real part and write the roots as

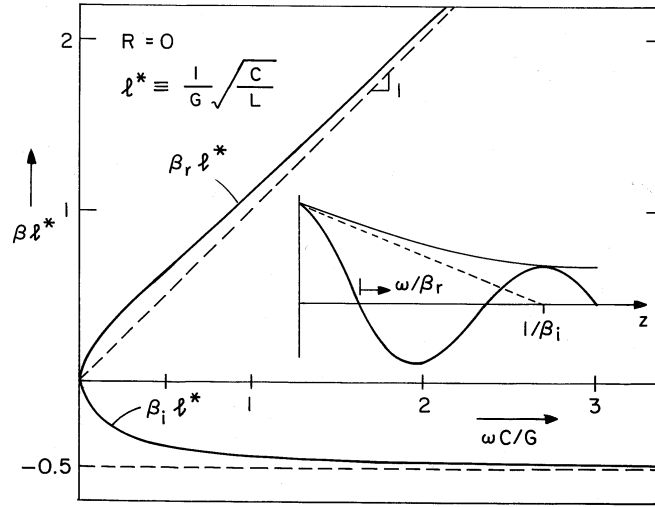


Fig. 14.7.2 Roots of (7) as functions of normalized ω . The real and imaginary parts, respectively, of the complex wave number β relate to the phase velocity and rate of decay of the wave, as shown.

$$k = \pm\beta; \quad \beta \equiv \sqrt{(\omega^2 LC - RG) - j\omega(RC + LG)}; \quad \text{Re } \beta > 0 \quad (8)$$

These roots, $k = k_r + jk_i$, are pictured as a function of frequency in Fig. 14.7.2. From (7), k^2 is in the lower half-plane. It follows that the value of k having a positive real part (defined as β) has a negative imaginary part.

These definitions take on physical significance when the solutions to (5) are written as

$$\hat{V} = \hat{V}_+ e^{-j\beta z} + \hat{V}_- e^{j\beta z} \quad (9)$$

because it is then clear that we have defined β so that V_+ represents a wave with points of constant phase propagating in the $+z$ direction. Note that because β_i is negative, this wave decays in the $+z$ direction, as shown in Fig. 14.7.2. Similarly, \hat{V}_- is the complex amplitude at $z = 0$ of a wave that decays in the $-z$ direction and has phases propagating in the $-z$ direction.¹⁰

In terms of the two coefficients \hat{V}_\pm , the current expression follows from substituting (9) into (6)

$$\hat{I} = \frac{1}{Z_o} (\hat{V}_+ e^{-j\beta z} - \hat{V}_- e^{j\beta z}) \quad (10)$$

where the complex characteristic impedance is now defined as

¹⁰ It is important not to generalize from this finding. The direction of propagation of points of constant phase (the phase propagation direction, PPG, is not, in general, indicative of the directions of propagation of the wave; i.e., a source positioned on an infinite line at $z = 0$ does not necessarily cause waves with positive PPG to go away from the source in the $+z$ direction and with negative PPG to go away in the $-z$ direction. The direction of propagation is usually determined by the direction of the group velocity (GV). In the presence of loss, waves with positive GV decay in the $+z$ -direction, with negative GV in the $-z$ -direction.

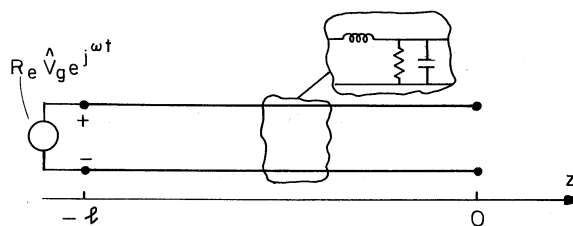


Fig. 14.7.3 Open circuit lossy line.

$$Z_o \equiv \frac{(R + j\omega L)}{j\beta} \quad (11)$$

Comparison of (9) and (10) with (14.5.5) and (14.5.6) shows that the impedance and reflection coefficient descriptions are applicable, provided we generalize β and Z_o to be the complex numbers given by (8) and (11). That these quantities are now complex is an inconvenience¹¹ and a warning that some ideas established for the ideal line need to be reexamined. For example, reasoning as in Sec. 14.5 shows that a pure resistance can no longer be used to match the line. Further, it is not possible to match the line at all frequencies with any finite number of lumped elements.

Example 14.7.1. Signal Attenuation on an Open Circuit Line

The lossy transmission line shown in Fig. 14.7.3 is open at the right and driven by a voltage source of complex amplitude V_g at the left. What is the voltage measured at the open circuit?

The open circuit at $z = 0$ requires that $I(0) = 0$, and hence [from (10)] that $V_+ = V_-$. Thus, the voltage, as given by (9), is

$$\hat{V} = \hat{V}_+(e^{-j\beta z} + e^{j\beta z}) = \hat{V}_g \frac{(e^{-j\beta z} + e^{j\beta z})}{(e^{j\beta l} + e^{-j\beta l})} \quad (12)$$

Here we have adjusted the coefficient \hat{V}_+ so that the voltage is \hat{V}_g at the left end, where the voltage source is connected. As a function of time, the voltage distribution is therefore

$$V(z, t) = \text{Re} \hat{V}_g \frac{(e^{-j\beta z} + e^{j\beta z})}{(e^{j\beta l} + e^{-j\beta l})} e^{j\omega t} \quad (13)$$

Much of the complicated phenomenon represented by this simple expression is encapsulated in the complex wave number. To illustrate, consider the voltage measured at $z = 0$, which from (13) has the complex amplitude

$$\hat{V}(0) = \frac{\hat{V}_g}{\cos \beta l} \quad (14)$$

If a calculator or computer is not available for evaluating the cosine of a complex number, then we can use the double-angle identity to write

$$\cos \beta l = \cos(\beta_r l + j\beta_i l) = \cos \beta_r l \cosh \beta_i l - j \sin \beta_r l \sinh \beta_i l \quad (15)$$

¹¹ Circumvented by having a calculator programmed to carry out operations on complex variables.

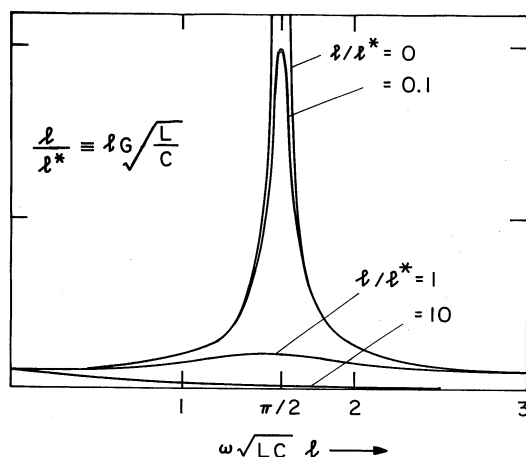


Fig. 14.7.4 Frequency response for open circuit lossy line.

For the case where all of the loss is due to the shunt conductance ($R = 0$), the frequency response is illustrated in Fig. 14.7.4. The four responses shown are for increasing amounts of loss, perhaps introduced by increasing G .

At very low frequencies, the output voltage simply follows the driving voltage. This is because we have considered the case where $R = 0$ and with the frequency so low that the inductor has no effect, the output terminals are connected to the source through a negligible impedance.

As the frequency is raised, consider first the response with no loss ($l/l^* = 0$). As the frequency approaches that required to make the line a quarter-wavelength long, the impedance of the line at the generator approaches zero and the current approaches infinity. This resonance condition results in the infinite response at $z = 0$. (As the frequency is raised further, these resonance conditions occur each time the frequency is such that the line has a length equal to a quarter-wavelength plus a multiple of a half-wavelength.) With the addition of a slight amount of loss ($l/l^* = 0.1$), the response is finite even under the resonance conditions. Further increasing the loss ($l/l^* = 1$) results in a response with a dull peak at the resonance point. Still larger losses ($l/l^* = 10$) bring in skin effect and monotonic attenuation of the voltage over the length of the line. Phenomena underlying this response are discussed in the next section.

14.8 UNIFORM AND TEM WAVES IN OHMIC CONDUCTORS ($R = 0$)

Transverse electromagnetic (TEM) waves that propagate in the z direction and are polarized in the x direction have electric and magnetic fields

$$\mathbf{E} = E_x(z, t)\mathbf{i}_x; \quad \mathbf{H} = H_y(z, t)\mathbf{i}_y \quad (1)$$

We consider here how waves having this form propagate through a material with not only uniform permittivity ϵ and permeability μ (as in Secs. 14.1–14.6) but now

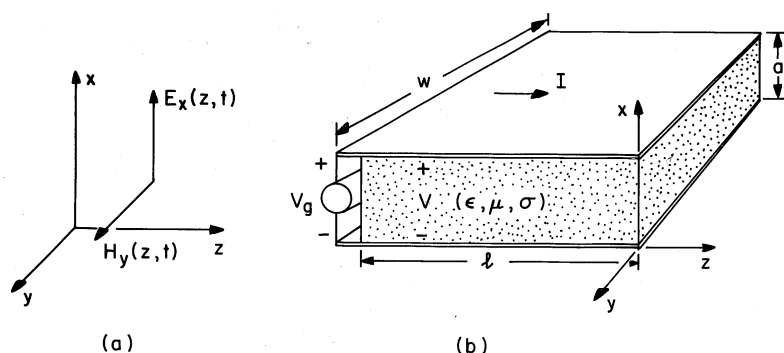


Fig. 14.8.1 (a) TEM fields in uniform lossy material. (b) Perfectly conducting electrodes with material having uniform σ as well as ϵ and μ between. With fringing field ignored, fields in the material have the transverse character of (a).

a uniform conductivity σ as well. As suggested by Fig. 14.8.1a, these fields might constitute plane waves in “infinite” media. They might also be the fields between the perfectly conducting planar electrodes of Fig. 14.8.1b. Our first objective in this section is to see that both the TEM fields in “infinite media” and on the “strip line” are described *exactly* by the distributed parameter model of Sec. 14.7 with $R = 0$. The ohmic loss introduces a conductance per unit length G .

With the introduction of fields having the form of (1) into the laws of Faraday and Ampère, only two of the six equations are not automatically satisfied. These are the x component of Ampère’s law with Ohm’s law used to express the conduction current

$$-\frac{\partial H_y}{\partial z} = \sigma E_x + \frac{\partial \epsilon E_x}{\partial t} \quad (2)$$

and the y component of Faraday’s law

$$\frac{\partial E_x}{\partial z} = -\frac{\partial \mu H_y}{\partial t} \quad (3)$$

Except for the conduction current, the first term on the right in (2), these are the same equations as featured in Secs. 14.1-14.6. They become the plane parallel transmission-line equations if (2) is multiplied by the plate width w and (3) is multiplied by $-a$, where a is the plate spacing

$$\frac{\partial I}{\partial z} = -GV - C \frac{\partial V}{\partial t} \quad (4)$$

$$\frac{\partial V}{\partial z} = -L \frac{\partial I}{\partial t} \quad (5)$$

where the current I and voltage V are

$$I \equiv K_z w = -H_y w; \quad V \equiv -E_x a \quad (6)$$

and

$$G = \frac{\sigma w}{a}; \quad C = \frac{\epsilon w}{a}; \quad L = \frac{\mu a}{w} \quad (7)$$

These are the same equations found for the distributed parameter line of Sec. 14.7 with $R = 0$. Thus, whether representing a plane wave in a uniform lossy material or the transmission-line filled with such a uniform medium, the distributed parameter model is “exact.”

From the point of view taken in Sec. 14.2, the geometry of the parallel conductors in the “strip line” is a special case. In the problems, the derivation of the transmission line equations given in Sec. 14.2 is generalized to include the effects of a uniformly conducting material in the space between the perfect conductors. Regardless of their cross-sectional geometry, so long as the pair of conductors are perfectly conducting and the material between them is uniform, the fields are exactly TEM and exactly represented by the distributed parameter model. Not only is $\sqrt{LC} = \sqrt{\mu\epsilon}$ (8.6.14), but so also is $C/G = \epsilon/\sigma$ (7.6.4), regardless of the cross-sectional geometry.

We now suppose that sinusoidal steady state conditions have been established. Then the voltage and current are represented by (14.7.9) and (14.7.10) with the wave number and characteristic impedance given by (14.7.8) and (14.7.11) with $R = 0$ and L, C , and G given by (7).

$$\beta = \sqrt{\omega^2\mu\epsilon - j\omega\mu\sigma} \quad (8)$$

$$Z_o = \frac{\omega\mu a}{w\beta} \quad (9)$$

Example 14.8.1. TEM Fields in a Lossy Material between Plane Parallel Plates Terminated in an Open Circuit

With an “open circuit” at $z = 0$ and driven by a voltage source at $z = -l$, the parallel plate configuration of Fig. 14.7.1b is equivalent to the open circuit transmission line of Example 14.7.1. With the understanding that β is now given by (8), it follows from (14.7.13) that

$$V = \text{Re } \hat{V}_g \frac{[e^{-j\beta l(z/l)} + e^{j\beta l(z/l)}]}{e^{j\beta l} + e^{-j\beta l}} e^{j\omega t} \quad (10)$$

Using the values of $\hat{V}_+ = \hat{V}_-$ implied by (14.7.12) in (14.7.10) results in the current distribution

$$I = \text{Re } \frac{\hat{V}_g}{Z_o} \frac{[e^{-j\beta l(z/l)} - e^{j\beta l(z/l)}]}{e^{j\beta l} + e^{-j\beta l}} e^{j\omega t} \quad (11)$$

where Z_o is evaluated using (9).

The voltage and current have been specified as a superposition of forward and backward waves, which, respectively, decay in the directions in which their phases propagate. The distribution of the square of the magnitude of V (of E_x) predicted by (10) (and hence of the time average dissipation density or time average electric energy density) is illustrated by Fig. 14.8.2. In this case, the electrical dissipation is small enough so that a standing wave pattern is evident. The wave propagating and decaying to the right interferes with the wave propagating and decaying to the left in such a way that the boundary condition at $z = 0$ is satisfied. In the neighborhood of $z = 0$, where the wave traveling to the left has not yet decayed appreciably, the two waves interfere to form the familiar standing wave pattern. However, at the left, the wave traveling to the left has largely decayed and so interferes with the wave

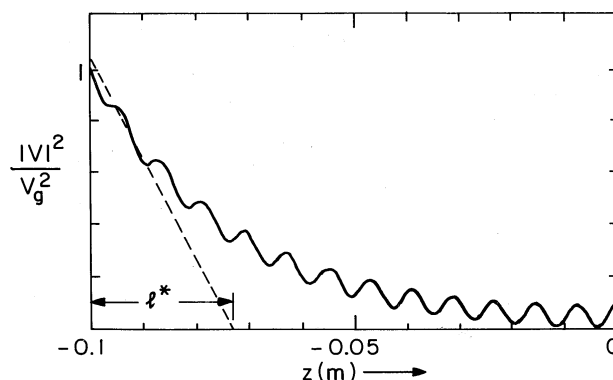


Fig. 14.8.2 Square of the magnitude of \hat{V} as a function of position z for a slightly damped electromagnetic wave. $\omega = 12 \times 10^{10}$ rad/s, $l = 0.1$ m, $\epsilon = \epsilon_0$, $\mu = \mu_0$, and $\sigma = 0.1$ S/m, so $\omega\epsilon/\sigma = \omega\tau_e = 10.6$ and $l^* = 0.0265$ m.

traveling to the right to produce no more than a ripple in the total field magnitude. Further insights concerning these field distributions will come from considering some limits of the dispersion equation discussed next.

The first and second terms under the radical in the dispersion equation, (8), represent the displacement and conduction current densities, respectively. The relative importance of these current densities is determined by the relationship between the frequency and the reciprocal charge relaxation time. This is evident if (8) is written as

$$\beta = \omega\sqrt{\mu\epsilon}\sqrt{1 - \frac{j}{\omega\tau_e}} \quad (12)$$

where $\tau_e \equiv \epsilon/\sigma$ is the charge relaxation time.

Displacement Current Much Greater Than Conduction Current:

$\omega\tau_e \gg 1$. In this limit, the waves are essentially electromagnetic, with some damping due to the finite conductivity. The second term under the radical in (12) is small compared to the first. Thus, the expression can be given a convenient approximation by using the first two terms in a binomial expansion.¹²

$$\beta \approx \omega\sqrt{\mu\epsilon} - \frac{j}{2l^*} \quad (13)$$

The natural distance over which the electromagnetic wave decays by $1/e$ is $2l^*$, where the *characteristic length* l^* is defined in (13) as

$$l^* \equiv \frac{1}{\sigma}\sqrt{\epsilon/\mu} \quad (14)$$

¹² With $x \equiv -j/\omega\tau_e$, $(1+x)^{1/2} \approx (1 + \frac{1}{2}x)$

Note that this length is the reciprocal of the intrinsic impedance conductivity product. With $\tau_e = C/G$, the dependence of β on ω given by (13) approximates the high-frequency range of Fig. 14.7.2.

In the case of Fig. 14.8.2, $\omega\epsilon/\sigma = 10.6$, so that the conditions for this low loss limit are met. Because the attenuation length for the electric field is $2l^*$, the attenuation length for the square of the magnitude of E_x is l^* , as shown in the figure, and the length of the system l is several times larger than the characteristic length l^* .

Conduction Current Much Greater Than Displacement Current:

$\omega\tau_e \ll 1$. In this limit, the effects of displacement current are ignored altogether so that the first term under the radical is neglected compared to the second, and the dispersion equation is approximated by

$$\beta \approx \sqrt{-j\omega\mu\sigma} = \frac{(1-j)}{\delta} \quad (15)$$

Here, $\delta \equiv \sqrt{2/\omega\mu\sigma}$ is the skin depth, familiar from Sec. 10.7.¹³ Thus, in this regime, the decay length is δ while the wavelength is $2\pi\delta$. The dependence of β on ω given by (15) approximates β in the low-frequency range of Fig. 14.7.2.

Example 14.8.2. Overview of TEM Fields in Open Circuit Transmission Line Filled with Lossy Material

Given the properties and dimensions of a simple system and a characteristic time for the dynamics, what are its dominant electromagnetic features? In this example, with the voltage source driving the system of Fig. 14.8.1b (so that the characteristic time is $1/\omega$), the system could be essentially a:

- (1) resistor, in which case E_x would be uniform (Sec. 7.2)
- (2) lossy capacitor, also with an essentially uniform E_x (Sec. 7.9)
- (3) distribution of inductors and resistors with the distribution of E_x governed by magnetic diffusion (Sec. 10.7)
- (4) lossy transmission line supporting slightly damped electromagnetic waves

With the objective of having a summary way of picturing these possibilities, we recognize that the field distributions [(10) and (11)] are exponential functions of $\beta l(z/l)$. Thus, βl encapsulates the field distribution. In terms of dimensionless parameters, $\omega\tau_e$ (representing the frequency) and l/l^* (representing the length), we write (12) as

$$\beta l = \sqrt{\omega\tau_e(\omega\tau_e - j)} \frac{l}{l^*} \quad (16)$$

and conclude that the field distributions are governed by two parameters, the length of the system relative to the characteristic length (l/l^*) and the frequency relative to

¹³ As defined by (10.7.2), the product of ω and the magnetic diffusion time based on this length, $\mu\sigma\delta^2$, is equal to 2.

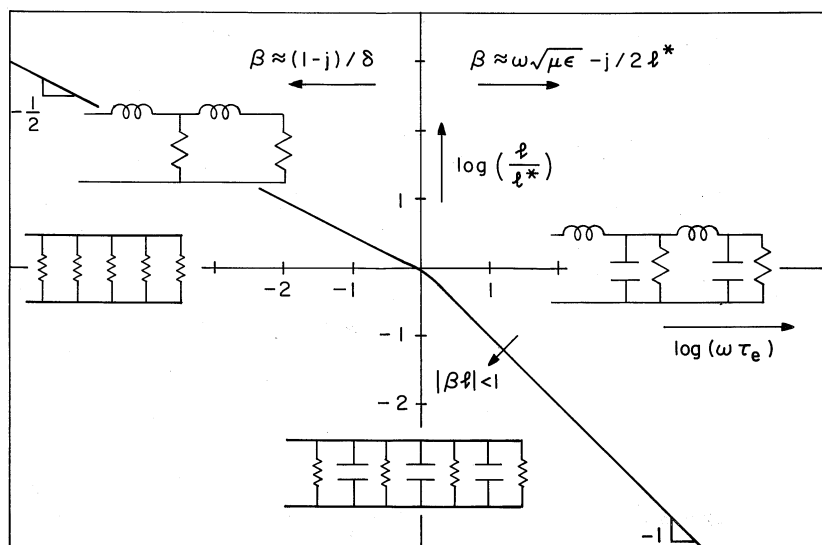


Fig. 14.8.3 In the length-frequency plane, regimes for TEM fields in material of uniform ϵ , μ , and σ between perfect conductors having length l (Fig. 14.8.1a). The length is normalized to $l^* = (\sigma\sqrt{\mu/\epsilon})^{-1}$ and the angular frequency to $\tau_e = \epsilon/\sigma$.

the reciprocal charge relaxation time ($\omega\tau_e$). The logs of these variables are the coordinates in Fig. 14.8.3. The origin of the plot is at the length equal to the characteristic length, l^* , and the angular frequency equal to the reciprocal charge relaxation time, $(\epsilon/\sigma)^{-1}$. These coordinates provide for a systematic overview of the electromagnetic regimes.

The approximate expressions for the wave number given by (13) and (15), respectively, apply to the right and left of the vertical axis, as indicated at the top of Fig. 14.8.3. It is tempting to jump to the conclusion that there are simply two regimes, the one to the right where the fields are composed of slightly damped electromagnetic waves, and the one to the left involving “skin-effect.” However, this is not the whole story, because it does not take into account the length of the system. It is really βl , and not β alone, that determines the field distribution between the plates.

Whether representing a slightly damped electromagnetic wave or magnetic diffusion (skin effect), a small value of βl means that there is little variation of the voltage over the length of the system. In the cases where $|\beta l| \ll 1$, the exponentials expressing the z dependence can be approximated by the first terms in a Taylor’s series. Thus, in this regime, the voltage (E_x) follows from (10) as being essentially uniform

$$V \approx \text{Re } \hat{V}_g e^{j\omega t} \quad (17)$$

and the current (H_y) given by (11) takes on an essentially linear distribution.

$$I \approx \frac{\hat{V}_g}{Z_o} (-j\beta l) \frac{z}{l} e^{j\omega t} = \text{Re } -\hat{V}_g \frac{w\sigma}{a} (1 + j\omega\tau_e) z e^{j\omega t} \quad (18)$$

The regime in Fig. 14.8.3 where this limit pertains, follows from the dispersion equation, (16).

$$|\beta l| = \frac{l}{l^*} (\omega \tau_e)^{1/2} [(\omega \tau_e)^2 + 1]^{1/4} \ll 1 \quad (19)$$

The line along which $\beta l = 1$ can be conveniently pictured by making this expression an equality, solving for l/l^* and taking the log.

$$\log\left(\frac{l}{l^*}\right) = -\frac{1}{2} \log(\omega \tau_e) - \frac{1}{4} \log[(\omega \tau_e)^2 + 1] \quad (20)$$

This makes it clear that for large values of $\omega \tau_e$, the line of demarcation has a slope of -1 , while for small values, its slope is $-1/2$. This line is shown in Fig. 14.8.3. In the region well to the southwest of this line, the electric field distribution is essentially uniform. The circuits drawn on the respective regions in Fig. 14.8.3 picture the four limiting cases.

In terms of this figure, picture what happens as the frequency is raised for systems that are larger than the matching length, $l \gg l^*$. In this case, raising the frequency follows a trajectory in the upper half-plane from the left to the right. With the frequency very low, the voltage and current distributions are approximated by (17) and (18). Because $\omega \tau_e \ll 1$, it follows from the latter equation that the system is essentially a resistor. As the line $\beta l = 1$ is approached, $\omega \tau_e$ is still small, so that effects of the displacement current are negligible. That the variation of the fields that comes into play is due to magnetic diffusion is clear from the appropriate limiting expression for β , (15). Indeed, the line $\beta l = 1$ in this quadrant approaches the line along which the angular frequency is equal to the reciprocal magnetic diffusion time based on the length l ,

$$\omega \tau_m = \omega \mu \sigma l^2 = 1 \quad (21)$$

as can be seen by rewriting this expression as

$$\log\left(\frac{l}{l^*}\right) = -\frac{1}{2} \log(\omega \tau_e) \quad (22)$$

In the neighborhood of this line, in the second quadrant where the magnetic diffusion line is shown (the distributed transmission line of Sec. 14.7 with $R = 0$ and $C = 0$), the system is magnetoquasistatic (MQS).

As the frequency is raised still further, the displacement current begins to come into effect. The wave number makes a transition from representing the heavily damped waves of magnetic diffusion to the slightly damped electromagnetic waves of the first quadrant.

Consider the contrasting nature of the system with its length much less than the characteristic length, $l \ll l^*$, as the frequency is raised.

As before, to the far left of the figure, the electric field is uniform and the current is that characteristic of a resistor. This regime, like that just above in the second quadrant, is one of quasi-steady conduction. In this regime, the fields are described by the steady conduction approximation which was the subject of the first half of Chap. 7.

By contrast with the situation in the upper half-plane, the fields now remain uniform until the angular frequency passes well beyond the reciprocal charge relaxation time, the vertical axis. Note that in this range, the voltage and current are those for a distribution of conductances shunting perfectly conducting plates, as shown in Fig. 14.8.3. Thus, all of the conductances and capacitances can be lumped together. Up to this frequency range, the system is electroquasistatic (EQS).

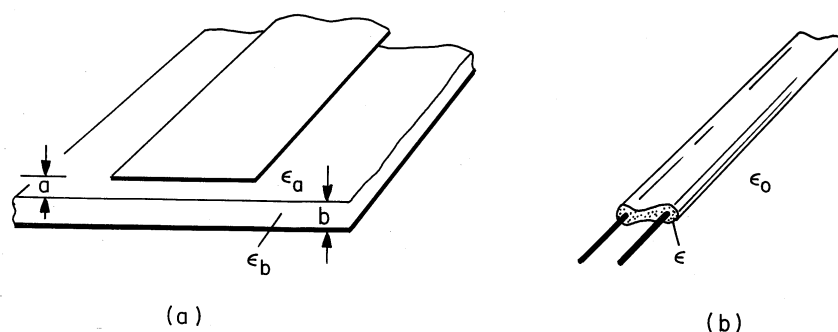


Fig. 14.8.4 (a) Strip line, used for microwave transmission on circuit boards and chips. (b) “Twin lead” commonly used for TV antennae.

As the frequency is raised still further, effects of magnetic induction come into play and conspire with the displacement current to create field distributions typical of electromagnetic waves. This happens in the range where $|\beta l| = 1$, because in this quadrant, the angular frequency is equal to the electromagnetic delay time based on the length of the system,

$$\omega\tau_{em} \equiv \omega\sqrt{\mu\epsilon}l = 1 \quad (23)$$

as can be seen by writing this expression as

$$\log\left(\frac{l}{l^*}\right) = -\log(\omega\tau_e) \quad (24)$$

In this frequency range and further to the right, the field distributions are those for slightly damped electromagnetic waves.

In summary, far to the left in Fig. 14.8.3, quasi-steady conduction prevails. The dynamic process that first comes into play as the frequency is raised is determined by the length of the system relative to the characteristic length. Systems large enough to be in the upper half-plane are in the MQS regime. Those small enough to be in the lower half-plane are in the EQS regime.

The distributed parameter transmission line is often used to represent the evolution of fields on pairs of conductors surrounded by inhomogeneous dielectrics. Practical examples are shown in Fig. 14.8.4, where the dielectric is piece-wise uniform. In these cases, even if the conductors can be represented as perfectly conducting, so that $R = 0$, the fields between the conductors are *not* exactly TEM. Completely transverse waves would propagate with different velocities in the two dielectric regions, and it would not be possible to match boundary conditions at the interfaces. Nevertheless, with C and G , respectively, taken as being the EQS capacitance and conductance per unit length of the open circuit conductors, and L the MQS inductance per unit length of the short circuit conductors, the distributed parameter line of Sec. 14.7 can provide an excellent model.

In cases where the material between the conductors is inhomogeneous, the distributed parameter model provides a good approximation of the principal mode of propagation, provided that the frequency is low enough to insure that the wavelength in the z direction is long compared to the cross-sectional dimensions. For

example, it is shown in the problems that there is a z -directed \mathbf{E} in the strip line of Fig. 14.8.4a, so the fields are not TEM. However, if one neglects fringing fields one can show that E_z is small compared to the transverse fields if

$$\frac{b(\beta a)}{a+b} \left| 1 - \frac{\epsilon_a}{\epsilon_b} \right| \ll 1 \quad (25)$$

Thus, the distributed parameter model is exact if the dielectric is uniform ($\epsilon_a = \epsilon_b$), and approximately correct if $\beta a = 2\pi a/\lambda$ is small enough to fulfill the inequality.

14.9 QUASI-ONE-DIMENSIONAL MODELS ($G = 0$)

The transmission line model of Sec. 14.7 can also represent the losses in the parallel conductors. With the conductors of finite conductivity, currents in the z direction cause a component of \mathbf{E} in that direction. Because the tangential \mathbf{E} is continuous at the surfaces of the conductors, this axial electric field extends into the insulating region between the conductors as well. We conclude that the fields are no longer exactly TEM when the conductor losses are finite.

Under what circumstances can the series distributed resistance R be used to represent the conductor losses? We will find that the conductivity must be sufficiently low so that the skin depth is large compared to the conductor thickness. One might expect that this model applies only to the case of large R . Interestingly, we find that this “constant resistance” model can remain valid even under circumstances where line losses are small, in the sense that the decay of a wave within a distance of the order of a wavelength is small. This occurs when $|\omega L| \gg R$, i.e., the effect of the distributed inductance is much larger than that of the series resistance. In the opposite extreme, where the effect of the series resistance is large compared to that of the inductance, the model represents EQS charge diffusion. A demonstration is used to exemplify physical situations modeled by this distributed R-C line. These include solid state electronic devices and physiological systems.

We conclude this section with a model that is appropriate if the skin depth is much less than the conductor thickness. By restricting the model to the sinusoidal steady state, the series distributed resistance R can be replaced by a “frequency dependent” resistance. This approximate model is typical of those used for representing losses in metallic conductors at radio frequencies and above.

We assume conductors in which the conduction current dominates the displacement current. In the sinusoidal steady state, this is true if

$$\frac{\omega\epsilon}{\sigma} \equiv \omega\tau_e \ll 1 \quad (1)$$

Thus, as the frequency is raised, the distribution of current density in the conductors is at first determined by quasi-stationary conduction (first half of Chap. 7) and then by the magnetic diffusion processes discussed in Secs. 10.3-10.7. That is, with the frequency low enough so that magnetic diffusion is essentially instantaneous, the current density is uniformly distributed over the conductor cross-sections. Intuitively, we should expect that the constant resistance R only represents conductor

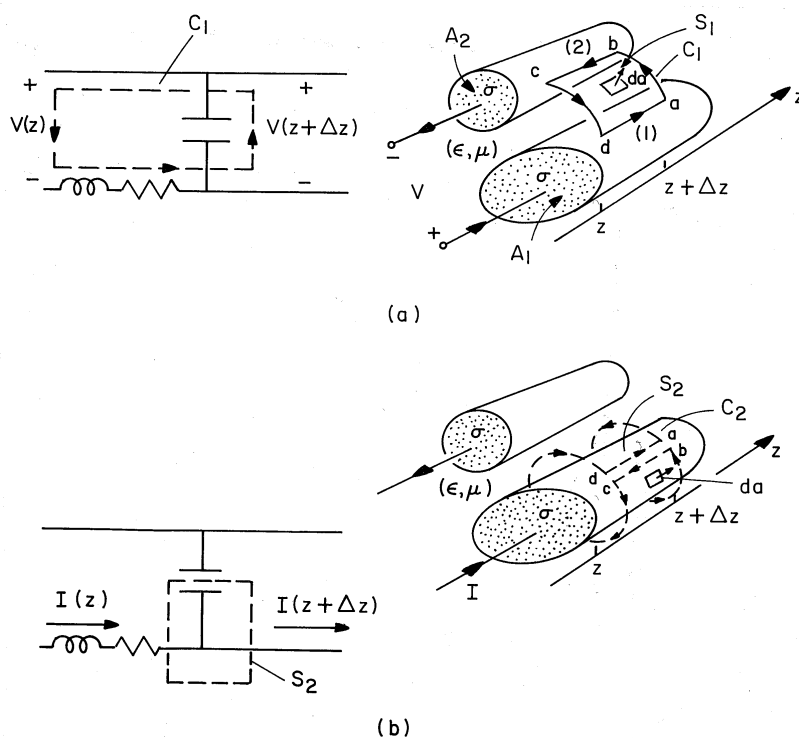


Fig. 14.9.1 (a) Faraday's integral law and, (b) Ampère's integral law applied to an incremental length Δz of line.

losses at frequencies sufficiently low so that the distribution of current density in the conductors does not depend on rates of change.

The equations used to describe the incremental circuit in Sec. 14.7 express the integral laws of Faraday and Ampère for incremental lengths of the transmission line. The "current loop equation" for loop C_1 in the circuit of Fig. 14.9.1a can be derived by applying Faraday's law to the surface S_1 enclosed by the contour C_1 , also shown in that figure.

$$\int_a^b \mathbf{E} \cdot d\mathbf{s} + \int_c^d \mathbf{E} \cdot d\mathbf{s} + E_z|_{(1)}\Delta z - E_z|_{(2)}\Delta z = -\frac{\partial}{\partial t} \int_{S_1} \mu \mathbf{H} \cdot d\mathbf{a} \quad (2)$$

With the line integrals between conductors defined as the voltages and the flux through the surface as $\Delta z LI$, this expression becomes

$$V(z + \Delta z) - V(z) + E_z|_{(1)}\Delta z - E_z|_{(2)}\Delta z = -\frac{\partial}{\partial t} \int_{S_1} \mu \mathbf{H} \cdot d\mathbf{a} \quad (3)$$

and in the limit where $\Delta z \rightarrow 0$, we obtain

$$\frac{\partial V}{\partial z} = -L \frac{\partial I}{\partial t} - E_z|_{(1)} + E_z|_{(2)} \quad (4)$$

The field equivalent of charge conservation for the circuit node enclosed by the surface S_2 in Fig. 14.9.1b is Ampère's integral law applied to the surface S_2 enclosed by the contour C_2 , also shown in that figure. Note that C_2 almost encircles one of the conductors with oppositely directed adjacent segments completing the z -directed parts of the contour. For a surface S_2 of incremental length Δz , Ampère's integral law requires that

$$\int_a^b \mathbf{H} \cdot d\mathbf{s} + \int_c^d \mathbf{H} \cdot d\mathbf{s} = \frac{\partial}{\partial t} \int_{S_2} \epsilon \mathbf{E} \cdot d\mathbf{a} \quad (5)$$

where the contributions from the oppositely directed legs in the z direction cancel. Ampère's integral law requires that the integral of $\mathbf{H} \cdot d\mathbf{s}$ on the contours essentially surrounding the conductor be the enclosed current I . Gauss' integral law requires that the surface integral of $\epsilon \mathbf{E} \cdot d\mathbf{a}$ be equal to $\Delta z CV$. Thus, (5) becomes

$$-I(z + \Delta z) + I(z) = C \Delta z \frac{\partial V}{\partial t} \quad (6)$$

and in the limit, the second transmission line equation.

$$\frac{\partial I}{\partial z} = -C \frac{\partial V}{\partial t} \quad (7)$$

If the current density is uniformly distributed over the cross-sectional areas A_1 and A_2 of the respective conductors, it follows that the current densities are related to the total current by

$$I = A_1 J_{z1} = -A_2 J_{z2} \quad (8)$$

In each conductor, $J_z = \sigma E_z$, so the axial electric fields required to complete (4) are related to I by

$$E_{z1} = \frac{J_{z1}}{\sigma_1} = \frac{I}{\sigma_1 A_1}; \quad E_{z2} = \frac{J_{z2}}{\sigma_2} = -\frac{I}{\sigma_2 A_2} \quad (9)$$

and indeed, the voltage equation is the same as for the distributed line,

$$\frac{\partial V}{\partial z} = -L \frac{\partial I}{\partial t} - RI \quad (10)$$

where the resistance per unit length has been found to be

$$R \equiv \frac{1}{\sigma_1 A_1} + \frac{1}{\sigma_2 A_2} \quad (11)$$

Example 14.9.1. Low-Frequency Losses on Parallel Plate Line

In the parallel plate transmission line shown in Fig. 14.9.2, the conductor thickness is b and the cross-sectional areas are $A_1 = A_2 = bw$. It follows from (11) that the resistance is

$$R = \frac{2}{bw\sigma} \quad (12)$$

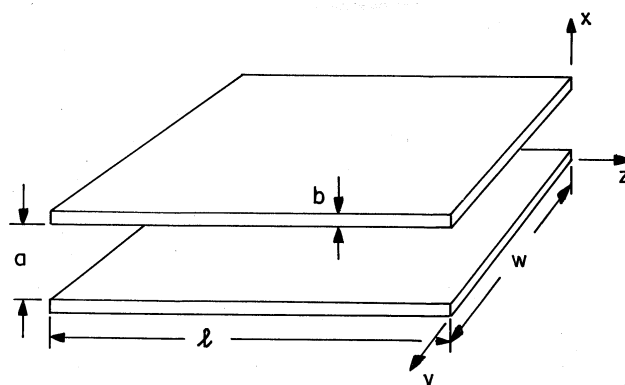


Fig. 14.9.2 Parallel plate transmission line with conductor thickness b that is small compared to skin depth.

Under the assumption that the conductor thickness, b , is much less than the plate spacing,¹⁴ a , the inductance per unit length is the same as found in Example 14.1.1, as is also the capacitance per unit length.

$$L = \frac{a\mu}{w}; \quad C = \frac{w\epsilon}{a} \quad (13)$$

As the frequency is raised, the current distribution over the cross-sections of the conductors becomes nonuniform when the skin depth δ (10.7.5) gets to be on the order of the plate thickness. Thus, for the model to be valid using the resistance given by (12),

$$\delta \equiv \sqrt{\frac{2}{\omega\mu\sigma}} \gg b \Rightarrow \omega\mu\sigma b \ll \frac{2}{b} \quad (14)$$

With this inequality we require that the effects of magnetic induction in determining the distribution of current in the conductors be negligible. Under what conditions are we justified in ignoring this effect of magnetic induction but nevertheless keeping that represented by the distributed inductance? Put another way, we ask if the inductive reactance $j\omega L$ can be large compared to the resistance R and still satisfy the condition of (14).

$$\omega L \gg R \Rightarrow \frac{2}{a} \ll \omega\mu\sigma b \quad (15)$$

Combined, these last two conditions require that

$$\frac{b}{a} \ll 1 \quad (16)$$

We conclude that as long as the conductor thicknesses are small compared to their spacing, R represents the loss over the full frequency range from dc to the frequency at which the current in the conductors ceases to be uniformly distributed. This is true because the time constant $\tau_m \equiv L/R = \mu\sigma ab$ that determines the frequency at which the resistance is equal to the inductive reactance¹⁵ is much larger than the magnetic diffusion time $\mu\sigma b^2$ based on the thickness of the conductors.

¹⁴ So that the magnetic energy stored in the plates themselves is negligible compared to that between the plates.

¹⁵ Familiar from Sec. 10.3.

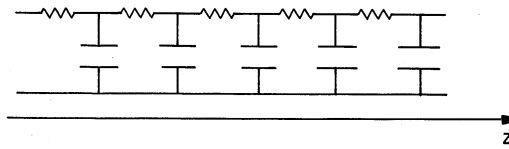


Fig. 14.9.3 Charge diffusion or R-C transmission line.

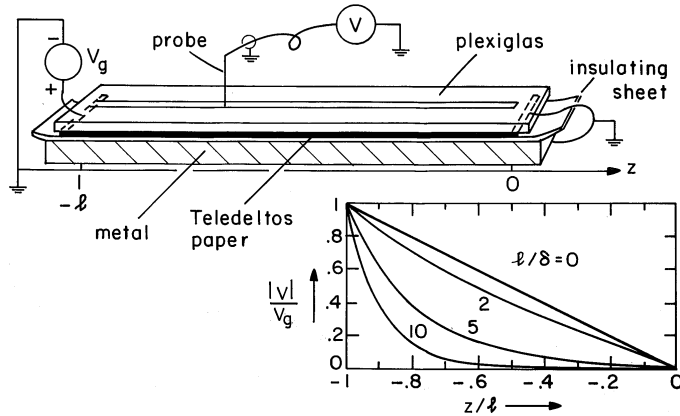


Fig. 14.9.4 Charge diffusion line.

Charge Diffusion Transmission Line. If the resistance is large enough so that the inductance has little effect, the lossy transmission line becomes an EQS model. The line is simply composed of the series resistance shunted by the distributed capacitance of Fig. 14.9.3. To see that the voltage (and hence charge) and current on this line are governed by the diffusion equation, (10) is solved for I , with L set equal to zero,

$$I = -\frac{1}{R} \frac{\partial V}{\partial z} \quad (17)$$

and that expression substituted into the z derivative of (7).

$$\frac{\partial^2 V}{\partial z^2} = RC \frac{\partial V}{\partial t} \quad (18)$$

By contrast with the charge relaxation process undergone by charge in a uniform conductor, the charge in this heterogeneous system diffuses. The distributed R-C line is used to model EQS processes that range from those found in neural conduction to relaxation in semiconductors. We can either view the solution of (17) and (18) as a special case from Sec. 14.7 or exploit the complete analogy to the magnetic diffusion processes described in Secs. 10.6 and 10.7.

Demonstration 14.9.1. Charge Diffusion Line

A simple demonstration of the charge diffusion line is shown in Fig. 14.9.4. A thin insulating sheet is sandwiched between a resistive sheet on top (the same Teledeltos paper used in Demonstration 7.6.2) and a metal plate on the bottom.

With sinusoidal steady state conditions established by means of a voltage source at $z = -l$ and a short circuit at the right, the voltage distribution is the analog of that described for magnetic diffusion in Example 10.7.1. The “skin depth” for the charge diffusion process is given by (10.7.5) with $\mu\sigma \rightarrow RC$.

$$\delta = \sqrt{\frac{2}{\omega RC}} \quad (19)$$

With this the new definition of δ , the magnitude of the voltage measured by means of the high-impedance voltmeter can be compared to the theory, plotted in Fig. 10.7.2. Typical values are $\epsilon = 3.5\epsilon_0$, $b\sigma = 4.5 \times 10^{-4}$ S (where $b\sigma$ is the surface conductivity of the conducting sheet), and $a = 25 \mu\text{m}$, in which case $RC = \epsilon/(b\sigma)a = 2.7 \times 10^{-3}$ sec/m² and $\delta \simeq 0.5$ m at a frequency of 500 Hz.

In the previous example, we found that the transmission line model is applicable provided that the conductor thicknesses were small compared to their spacing and to the skin-depth. That the model could be self-consistent from dc up to frequencies at which the inductive impedance dominates resistance is in part attributable to the plane parallel geometry.

To see this, consider a transmission line composed of a circular cylindrical conductor and a thin sheet, as shown in Fig. 8.6.7. In Demonstration 8.6.1, it was found that the condition $\mathbf{n} \cdot \mathbf{B} = 0$ on the conductor surfaces is met at frequencies for which the skin depth is far *greater* than the thickness of the thin sheet conductor. The examples of Sec. 10.4 show why this is possible. The effective magnetic diffusion time that determines the frequency at which currents in the conducting sheet make a transition from a quasi-stationary distribution to one consistent with $\mathbf{n} \cdot \mathbf{B} = 0$ is $\mu\sigma\Delta l$, where Δ is the thickness of the conductor and l is the distance between conductors. This is also the L/R time constant governing the transition from resistance to inductance domination in the distributed electrodynamic model. We conclude that, even though the current may be essentially uniform over the conductor cross section, as the frequency changes from dc to the inductance dominated range, the current can shift its distribution over the conductor surface. Thus, in non-planar geometries, the constant R model can be inadequate even over a frequency range where the skin depth is large compared to the conductor thickness.

Skin Depth Small Compared to All Dimensions of Interest. In transmission lines used at radio frequencies and higher, it is usual for the skin depth to be much less than the conductor thickness, $\delta \ll b$. In the case of Fig. 14.9.2, $2 \ll \omega\mu\sigma b^2$. Provided that $a > b$, it follows from (15) that the inductive reactance dominates resistance. Although the line is then very nearly ideal, it is often long enough so that losses cannot be neglected. We therefore conclude this section by developing a model, restricted to the sinusoidal steady state, that accounts for losses when the skin depth is small compared to all dimensions of interest.

In this case, the axial conduction currents are confined to within a few skin depths of the conductor surfaces. Within a few skin depths, the tangential magnetic field decays from its value at the conductor surface to zero. Because the magnetic field decays so rapidly along a coordinate perpendicular to a given point on the conductor surface, the effects on the magnetic diffusion of spatial variations along

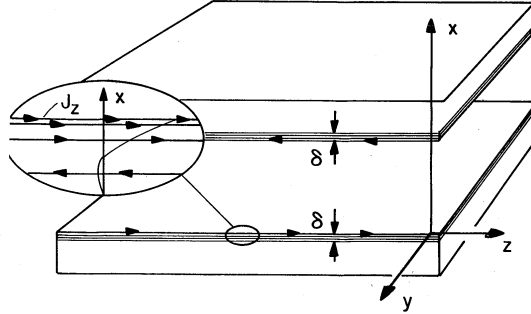


Fig. 14.9.5 Parallel plate transmission line with conductors that are thick compared to the skin depth.

the conductor surface are negligible. For this reason, fields in the conductors can be approximated by the one-dimensional magnetic diffusion process described in Sec. 10.7. The following example illustrates this concept.

Example 14.9.2. High-Frequency Losses on Parallel Plate Line

The parallel plate transmission line is shown again in Fig. 14.9.5, this time with the axial current distribution in the conductors in thin regions on the inner surfaces of the conductors rather than uniform. In the conductors, the displacement current is negligible, so that the magnetic field is governed by the magnetic diffusion equation, (10.5.8). In the sinusoidal steady state, the y component of this equation requires that

$$\frac{1}{\mu\sigma} \left[\frac{\partial^2 \hat{H}_y}{\partial x^2} + \frac{\partial^2 \hat{H}_y}{\partial z^2} \right] = -j\omega \hat{H}_y \quad (20)$$

The first term on the left is of the order of $H_y/(\delta)^2$, while the second is of the order of $H_y k^2 = H_y (2\pi/\lambda)^2$ [where λ is the wavelength in the axial (z) direction]. Thus, the derivative with respect to z can be ignored compared to that with respect to x , provided that

$$\frac{1}{\delta^2} \gg k^2 \Rightarrow \delta \ll \frac{\lambda}{2\pi} \quad (21)$$

In this case, (20) becomes the one-dimensional magnetic diffusion equation studied in Sec. 10.7. In the lower conductor, the magnetic field diffuses in the $-x$ direction, so the appropriate solution to (20) is

$$\hat{H}_y = \hat{H}_o e^{(1+j)x/\delta} \quad (22)$$

where H_o is the magnetic field intensity at the surface of the lower conductor [see (10.7.8)]. Ampère's law gives the current density associated with this field distribution

$$\hat{J}_z = \frac{\partial \hat{H}_y}{\partial x} = \frac{\hat{H}_o (1+j)}{\delta} e^{(1+j)x/\delta} \quad (23)$$

It follows from either integrating this expression over the cross-section of the lower conductor or appealing to Ampère's integral law that the total current in the lower conductor is

$$\hat{I} = w \int_{-\infty}^0 \hat{J}_z dx = w \hat{H}_o \quad (24)$$

The axial electric field intensity at the surface of the lower conductor can now be written in terms of this total current by first using Ohm's law and the current density of (23) evaluated at the surface and then using (24) to express this field in terms of the total current.

$$\hat{E}_z(0) = \frac{\hat{J}_z(0)}{\sigma} = \frac{\hat{I}(1+j)}{w\sigma\delta} \quad (25)$$

A similar derivation gives an axial electric field at the surface of the upper conductor that is the negative of this result. Thus, we can complete the sinusoidal steady state version of the voltage transmission-line equation, (4).

$$\frac{d\hat{V}}{dz} = - \left[j\omega L + \frac{2(1+j)}{w\sigma\delta} \right] \hat{I} \quad (26)$$

Because the magnetic energy stored within the conductor is usually negligible compared to that in the region between conductors,

$$\omega L \gg \frac{2}{w\sigma\delta} \quad (27)$$

and (26) becomes the first of the two sinusoidal steady state transmission line equations.

$$\frac{d\hat{V}}{dz} = - \left(j\omega L + \frac{2}{w\sigma\delta} \right) \hat{I} \quad (28)$$

The second follows directly from (7).

$$\frac{d\hat{I}}{dz} = -j\omega C\hat{V} \quad (29)$$

Comparison of these expressions with those describing the line operating with the conductor thickness much less than the skin depth, (10) and (7), shows that here there is an equivalent distributed resistance.

$$R_{eq} = \frac{2}{w\sigma\delta} = \frac{1}{w} \sqrt{\frac{2\omega\mu}{\sigma}} \quad (30)$$

(Here, μ is the permeability of the conductor, not of the region between conductors.) Note that this is the series dc resistance of conductors having width w and thickness δ . Because δ is inversely proportional to the square root of the frequency, this equivalent resistance increases with the square root of the frequency.

14.10 SUMMARY

The theme in this chapter has been the transmission line. It has been used to represent the evolution of electromagnetic fields through structures generally comprised of a pair of "conductors" embedded in a less conducting, and often highly insulating, medium. We have confined ourselves to systems that are uniform in the direction of evolution, the z direction.

If the conductors can be regarded as perfectly conducting, and the medium in which they are embedded as having uniform permeability, permittivity, and conductivity, the fields are exactly TEM, regardless of the cross-sectional geometry. The relevant laws and distributed parameter model are summarized in Table 14.10.1. Identification of variables as illustrated in the table make the transmission line exactly *equivalent* to a plane wave. Whether L , C , or G represent fields propagating along the conductors or a plane wave, $LC = \mu\epsilon$ and $C/G = \epsilon/\sigma$.

Much of this chapter is devoted to describing the limit where the conductors are not only perfect, but the medium has negligible conductivity ($G = 0$). Transients on this “ideal” transmission line are described by using the relations summarized in Table 14.10.2. The voltage and current at any position and time (z, t) are superpositions of wave components that propagate with the velocity c . These forward and backward wave components are, respectively, invariant on lines in the $z - t$ plane of constant α and β . Along those lines originating on initial conditions, the wave components are as summarized in the second row of the table. The last two rows summarize how the reflected wave component is determined from the incident component at two common terminations.

A summary of the relations used to describe the ideal line in the sinusoidal steady state is given in Table 14.10.3. Because it has a magnitude that is constant and a phase that increases linearly with z , the evolution of voltage and current and of their ratio, the impedance $Z(z)$, is conveniently pictured in terms of the complex reflection coefficient, $\Gamma(z)$. Relations and the complex Γ plane are illustrated in the first row. The mappings of the impedance and of the admittance onto this plane, respectively, are summarized by the second and third rows. Because the magnitude of Γ is constant over a uniform length of line, the trajectory of $Z(z)$ or $Y(z)$ is on a circle of constant radius in the directions of the generator or the load, as indicated. These Smith charts give a convenient overview of how the impedance and admittance vary with position.

In Sec. 14.7, a shunt conductance per unit length, G , (to represent losses in the material between the transmission line conductors) and a series resistance per unit length, R , (for losses in the conductors themselves) was added to the distributed parameter transmission line representation. For the limiting case where the conductors were infinitely conducting, $R = 0$, and the material between of uniform properties, the fields represented by the line were exactly TEM. In the case where the material properties did vary over the cross section, the distributed parameter picture provided a useful model for the line provided that the wavelength was long compared to the cross-sectional dimensions. In specific terms, this model gave the opportunity to consider the dynamical processes considered in Chaps. 7, 10, and 12 (charge relaxation, magnetic diffusion and electromagnetic wave propagation, respectively) in one self consistent situation. What was learned will be generalized in the review of the processes given in Secs. 15.3–15.4.

In Sec. 14.9, where $G = 0$ but R was finite, the specific objective was to understand how the transmission line concept could be used to approximate conductor losses. A broader objective was to again illustrate the use of the distributed parameter line as a model, representing the fields at frequencies sufficiently low so that the wavelength is long compared with the transverse dimensions.

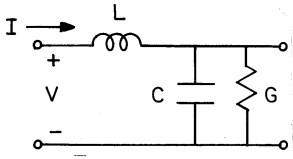
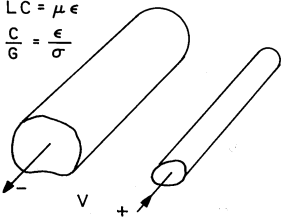
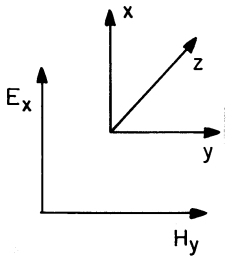
TABLE 14.10.1 TRANSMISSION LINE EQUIVALENTS		
$\frac{\partial I}{\partial z} = -C \frac{\partial V}{\partial t} - GV$	(14.8.4)	
$\frac{\partial V}{\partial z} = -L \frac{\partial I}{\partial t}$	(14.8.5)	
<div style="display: flex; align-items: center;"> <div style="margin-right: 20px;"> $LC = \mu \epsilon$ $\frac{C}{G} = \frac{\epsilon}{\sigma}$ </div>  </div>	$I \rightarrow H_y$ $V \rightarrow E_x$	
	$C \rightarrow \epsilon = n^2 \epsilon_0$ $L \rightarrow \mu$ $\frac{C}{G} \rightarrow \epsilon / \sigma$	

TABLE 14.10.2 WAVE TRANSIENTS		
$V = V_+(\alpha) + V_-(\beta)$	(14.3.9)	
$I = \frac{1}{Z_o}(V_+(\alpha) - V_-(\beta))$	(14.3.10)	
$\alpha = z - ct; \quad \beta = z + ct$	(14.3.11)	
$Z_o = \sqrt{L/C}$	(14.3.12)	
$c = 1/\sqrt{LC}$	(14.3.1)	
$V_+ = \frac{1}{2}(V_i + Z_o I_i)$	(14.3.18)	
$V_- = \frac{1}{2}(V_i - Z_o I_i)$	(14.3.19)	
$V_- = V_+ \frac{\left(\frac{R_L}{Z_o} - 1\right)}{\left(\frac{R_L}{Z_o} + 1\right)}$	(14.4.8)	
$V_+ = \frac{V_g}{\left(\frac{R_g}{Z_o} + 1\right)} + V_- \frac{\left(\frac{R_g}{Z_o} - 1\right)}{\left(\frac{R_g}{Z_o} + 1\right)}$	(14.4.10)	

TABLE 14.10.3
SINUSOIDAL-STEADY-STATE ($R = 0, G = 0$)

$\hat{V} = \hat{V}_+ e^{-j\beta z} [1 + \Gamma(z)]$ $\hat{I} = \frac{\hat{V}_+ e^{-j\beta z}}{Z_o} [1 - \Gamma(z)]$ $\Gamma \equiv \frac{\hat{V}_-}{\hat{V}_+} e^{j2\beta z}$ $Z_o = \sqrt{L/C}$ $\beta = \omega\sqrt{LC}$	<p>(14.5.5)</p> <p>(14.5.6)</p> <p>(14.6.2)</p> <p>(14.3.12)</p> <p>(14.5.5)</p>	
$\frac{Z(z)}{Z_o} = \frac{1 + \Gamma(z)}{1 - \Gamma(z)} \equiv r + jx$ $\Gamma = \frac{\frac{Z}{Z_o} - 1}{\frac{Z}{Z_o} + 1}$	<p>(14.6.1)</p> <p>(14.6.3)</p>	
$\frac{Y(z)}{Y_o} = \frac{1 - \Gamma(z)}{1 + \Gamma(z)} = g + jy$ $\Gamma = \frac{1 - \frac{Y}{Y_o}}{1 + \frac{Y}{Y_o}}$ $Y_o = \sqrt{C/L}$	<p>(14.6.12)</p>	

PROBLEMS

14.1 Distributed Parameter Equivalent Models

- 14.1.1 The “strip line” shown in Fig. P14.1.1 is an example where the fields are *not* exactly TEM. Nevertheless, wavelengths long compared to a and b , the distributed parameter model is applicable. The lower perfectly conducting plate is covered by a planar perfectly insulating layer having properties $(\epsilon_b, \mu_b = \mu_0)$. Between this layer and the upper electrode is a second perfectly insulating material having properties $(\epsilon_a, \mu_a = \mu_0)$. The width w is much greater than $a + b$, so fringing fields can be ignored. Determine L and C and hence the transmission line equations. Show that $LC \neq \mu\epsilon$ unless $\epsilon_a = \epsilon_b$.

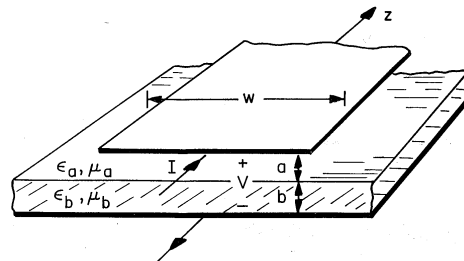


Fig. P14.1.1

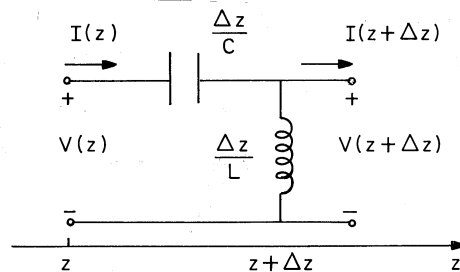


Fig. P14.1.2

- 14.1.2 An incremental section of a “backward wave” transmission line is as shown in Fig. P14.1.2. The incremental section of length Δz shown has a reciprocal capacitance per unit length $\Delta z C^{-1}$ and reciprocal inductance per unit length $\Delta z L^{-1}$. Show that, by contrast with (4) and (5), in this case the transmission line equations are

$$L \frac{\partial^2 I}{\partial t \partial z} = -V; \quad C \frac{\partial^2 V}{\partial t \partial z} = -I \quad (a)$$

14.2 Transverse Electromagnetic Waves

14.2.1* For the coaxial configuration of Fig. 14.2.2b,

(a) Show that, defined as zero on the outer conductor, A_z and Φ are

$$A_z = -\mu I \ln(r/a)/2\pi; \quad \Phi = -\lambda_l \ln(r/a)/2\pi\epsilon \quad (a)$$

where λ_l is the charge per unit length on the inner conductor.

(b) Using these expressions, show that the L and C needed to complete the transmission line equations are

$$L = \frac{\mu}{2\pi} \ln\left(\frac{a}{b}\right); \quad C = 2\pi\epsilon / \ln\left(\frac{a}{b}\right) \quad (b)$$

and hence that $LC = \mu\epsilon$.

14.2.2 A transmission line consists of a conductor having the cross-section shown in Fig. P4.7.5 adjacent to an L -shaped return conductor comprised of “ground planes” in the planes $x = 0$ and $y = 0$, intersecting at the origin. Assuming that the region between these conductors is free space, what are the transmission line parameters L and C ?

14.3 Transients on Infinite Transmission Lines

14.3.1 Show that the characteristic impedance of a coaxial cable (Prob. 14.2.1) is

$$Z_o = \sqrt{\mu/\epsilon} \ln(a/b)/2\pi \quad (a)$$

For a dielectric having $\epsilon = 2.5\epsilon_o$ and $\mu = \mu_o$, evaluate Z_o for values of $a/b = 2, 10, 100$, and 1000 . Would it be reasonable to design such a cable to have $Z_o = 1K\Omega$?

14.3.2 For the parallel conductor line of Fig. 14.2.2 in free space, what value of l/R should be used to make $Z_o = 300$ ohms?

14.3.3 The initial conditions on an infinite line are $V = 0$ and $I = I_p$ for $-d < z < d$ and $I = 0$ for $z < -d$ and $d < z$. Determine $V(z, t)$ and $I(z, t)$ for $0 < t$, presenting the solution graphically, as in Fig. 14.3.2.

14.3.4 On an infinite line, when $t = 0$, $V = V_o \exp(-z^2/2a^2)$, and $I = 0$, determine analytical expressions for $V(z, t)$ and $I(z, t)$.

14.3.5* In the energy conservation theorem for a transmission line, (14.2.19), VI is the power flow. Show that at any location, z , and time, t , it is correct to

think of power flow as the superposition of power carried by the + wave in the +z direction and – wave in the –z direction.

$$VI = \frac{1}{Z_o} [V_+^2 - V_-^2] \quad (a)$$

- 14.3.6** Show that the traveling wave solutions of (2) are not solutions of the equations for the “backward wave” transmission line of Prob. 14.1.2.

14.4 Transients on Bounded Transmission Lines

- 14.4.1** A transmission line, terminated at $z = l$ in an “open circuit,” is driven at $z = 0$ by a voltage source V_g in series with a resistor, R_g , that is matched to the characteristic impedance of the line, $R_g = Z_o$. For $t < 0$, $V_g = V_o = \text{constant}$. For $0 < t$, $V_g = 0$. Determine the distribution of voltage and current on the line for $0 < t$.
- 14.4.2** The transient is to be determined as in Prob. 14.4.1, except the line is now terminated at $z = l$ in a “short circuit.”
- 14.4.3** The transmission line of Fig. 14.4.1 is terminated in a resistance $R_L = Z_o$. Show that, provided that the voltage and current over the length of the line are initially zero, the line has the same effect on the circuit connected at $z = 0$ as would a resistance Z_o .
- 14.4.4** A transmission line having characteristic impedance Z_a is terminated at $z = l + L$ in a resistance $R_a = Z_a$. At the other end, where $z = l$, it is connected to a second transmission line having the characteristic impedance Z_b . This line is driven at $z = 0$ by a voltage source $V_g(t)$ in series with a resistance $R_b = Z_b$. With $V_g = 0$ for $t < 0$, the driving voltage makes a step change to $V_g = V_o$, a constant voltage. Determine the voltage $V(0, t)$.
- 14.4.5** A pair of transmission lines is connected as in Prob. 14.4.4. However, rather than being turned on when $t = 0$, the voltage source has been on for a long time and when $t = 0$ is suddenly turned off. Thus, $V_g = V_o$ for $t < 0$ and $V_g = 0$ for $0 < t$. The lines have the same wave velocity c . Determine $V(0, t)$. (Note that, by contrast with the situation in Prob. 14.4.4, the line having characteristic impedance Z_a now has initial values of voltage and current.)
- 14.4.6** A transmission line is terminated at $z = l$ in a “short” and driven at $z = 0$ by a current source $I_g(t)$ in parallel with a resistance R_g . For $0 < t < T$, $I_g = I_o = \text{constant}$, while for $t < 0$ and $T < t$, $I_g = 0$. For $R_g = Z_o$, determine $V(0, t)$.

14.4.7 With R_g not necessarily equal to Z_o , the line of Prob. 14.4.6 is driven by a step in current; for $t < 0$, $I_g = 0$, while for $0 < t$, $I_g = I_o = \text{constant}$.

- (a) Using an approach suggested by Example 14.4.3, determine the current $I(0, t)$.
- (b) If the transmission line is MQS, the system can be represented by a parallel inductor and resistor. Find $I(0, t)$ assuming such a model.
- (c) Show that in the limit where the round-trip transit time $2l/c$ is short compared to the time $\tau = lL/R_g$, the current $I(0, t)$ found in (a) approaches that predicted by the MQS model.

14.4.8 The transmission line shown in Fig. P14.4.8 is terminated in a series load resistance, R_L , and capacitance C_L .

- (a) Show that the algebraic relation between the incident and reflected wave at $z = l$, given by (8) for the load resistance alone, is replaced by the differential equation at $z = l$

$$Z_o C_L \left(\frac{R_L}{Z_o} + 1 \right) \frac{dV_-}{dt} + V_- = Z_o C_L \left(\frac{R_L}{Z_o} - 1 \right) \frac{dV_+}{dt} + V_+ \quad (a)$$

which can be solved for the reflected wave $V_-(l, t)$ given the incident wave $V_+(l, t)$.

- (b) Show that if the capacitor voltage is V_c when $t = 0$, then

$$V_-(l, 0) = \frac{V_c}{\left(\frac{R_L}{Z_o} + 1 \right)} + V_+(l, 0) \frac{\left(\frac{R_L}{Z_o} - 1 \right)}{\left(\frac{R_L}{Z_o} + 1 \right)} \quad (b)$$

- (c) Given that $V_g(t) = 0$ for $t < 0$, $V_g(t) = V_o = \text{constant}$ for $0 < t$, and that $R_g = Z_o$, determine $V(0, t)$.

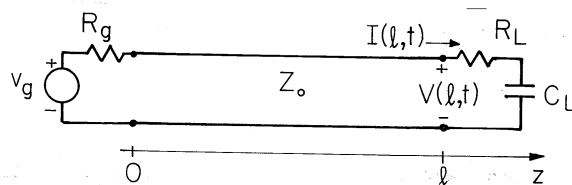


Fig. P14.4.8

14.5 Transmission Lines in the Sinusoidal Steady State

14.5.1 Determine the impedance of a quarter-wave section of line that is terminated, first, in a load capacitance C_L , and second, in a load inductance L_L .

14.5.2 A line having length l is terminated in an open circuit.

- (a) Determine the line admittance $Y(-l)$ and sketch it as a function of $\omega l/c$.
- (b) Show that the low-frequency admittance is that of a capacitor lC .

14.5.3* A line is matched at $z = 0$ and driven at $z = -l$ by a voltage source $V_g(t) = V_o \sin(\omega t)$ in series with a resistance equal to the characteristic impedance of the line. Thus, the line is as shown in Fig. 14.4.5 with $R_g = Z_o$. Show that in the sinusoidal steady state,

$$V = \operatorname{Re} \frac{1}{2} \hat{V}_g e^{-j\beta(z+l)} e^{j\omega t}; \quad I = \operatorname{Re} \frac{1}{2Z_o} \hat{V}_g e^{-j\beta(z+l)} e^{j\omega t}$$

where $\hat{V}_g \equiv -jV_o$.

14.5.4 In Prob. 14.5.3, the drive is zero for $t < 0$ and suddenly turned on when $t = 0$. Thus, for $0 < t$, $V_g(t)$ is as in Prob. 14.5.3. With the solution written in the form of (1), where $V_s(z, t)$ is the sinusoidal steady state solution found in Prob. 14.5.3, what are the initial and boundary conditions on the transient part of the solution? Determine $V(z, t)$ and $I(z, t)$.

14.6 Reflection Coefficient Representation of Transmission Lines

14.6.1* The normalized load impedance is $Z_L/Z_o = 2 + j2$. Use the Smith chart to show that the impedance of a quarter-wave line with this termination is $Z/Z_o = (1 - j)/4$. Check this result using (20).

14.6.2 For a normalized load impedance $Z_L/Z_o = 2 + j2$, use (3) to evaluate the reflection coefficient, $|\Gamma|$, and hence the VSWR, (10). Use the Smith chart to check these results.

14.6.3 For the system shown in Fig. 14.6.6a, the load admittance is $Y_L = 2Y_o$. Determine the position, l , and length, l_s , of a shorted stub, also having the characteristic admittance Y_o , that matches the load to the line.

14.6.4 In practice, it may not be possible or convenient to control the position l of the stub, as required for single stub matching of a load admittance Y_L to a line having characteristic admittance Y_o . In that case, a “double stub” matching approach can be used, where two stubs at arbitrary locations but with adjustable lengths are used. At the price of restricting the range of loads that can be matched, suppose that the first stub is attached in parallel with the load and shorted at length l_1 , and that the second stub is shorted at length l_2 and connected in parallel with the line at a given distance l from the load. The stubs have the same characteristic admittance as the line. Describe how, given the load admittance and the distance l to the second stub, the lengths l_1 and l_2 would be designed to match the load to the line. (Hint: The first stub can be adjusted in length to locate

the effective load anywhere on the circle on the Smith chart having the normalized conductance g_L of the load.) Demonstrate for the case where $Y_L = 2Y_o$ and $l = 0.042\lambda$.

- 14.6.5** Use the Smith chart to obtain the VSWR on the line to the left in Fig. 14.5.3 if the load resistance is $R_L/Z_o = 2$ and $Z_o^a = 2Z_o$. (Hint: Remember that the impedance of the Smith chart is normalized to the characteristic impedance at the position in question. In this situation, the lines have different characteristic impedances.)

14.7 Distributed Parameter Equivalents and Models with Dissipation

- 14.7.1** Following the steps exemplified in Section 14.1, derive (1) and (2).

- 14.7.2** For Example 14.7.1,

- (a) Determine $I(z, t)$.
- (b) Find the impedance at $z = -l$.
- (c) In the long wave limit, $|\beta l| \ll 1$, what is this impedance and what equivalent circuit does it imply?

- 14.7.3** The configuration is as in Example 14.7.1 except that the line is shorted at $z = 0$. Determine $V(z, t)$ and $I(z, t)$, and hence the impedance at $z = -l$. In the long wave limit, $|\beta l| \ll 1$, what is this impedance and what equivalent circuit does it imply?

- 14.7.4*** Following steps suggested by the derivation of (14.2.19),

- (a) Use (1) and (2) to derive the power theorem

$$-\frac{\partial}{\partial z}(VI) = \frac{\partial}{\partial t} \left(\frac{1}{2}CV^2 + \frac{1}{2}LI^2 \right) + I^2R + V^2G \tag{a}$$

- (b) The product of two sinusoidally varying quantities is a constant (time average) part plus a part that varies sinusoidally at twice the frequency. In complex notation,

$$\text{Re}\hat{A}e^{j\omega t}\text{Re}\hat{B}e^{j\omega t} = \frac{1}{2}\text{Re}\hat{A}\hat{B}^* + \frac{1}{2}\text{Re}\hat{A}\hat{B}e^{2j\omega t} \tag{b}$$

Use (11.5.7) to prove this identity.

- (c) Show that, in describing the sinusoidal steady state, the time average of the power theorem becomes

$$-\frac{d}{dz} \left(\frac{1}{2}\text{Re}\hat{V}\hat{I}^* \right) = \frac{1}{2}\text{Re}(\hat{I}\hat{I}^*R + \hat{V}\hat{V}^*G) \tag{c}$$

Show that for Example 14.7.1, it follows that the time average power input is equal to the integral over the length of the time average power dissipation per unit length.

$$\frac{1}{2}\text{Re}\hat{V}\hat{I}^*|_{z=-l} = \int_{-l}^0 \frac{1}{2}\text{Re}(\hat{I}\hat{I}^*R + \hat{V}\hat{V}^*G)dz \quad (d)$$

- (d) Evaluate the time average input power on the left in this relation and the integral of the time average dissipation per unit length on the right and show that they are indeed equal.

14.8 Uniform and TEM Waves in Ohmic Conductors

- 14.8.1** In the general TEM configuration of Fig. 14.2.1, the material between the conductors has uniform conductivity, σ , as well as uniform permittivity, ϵ . Following steps like those leading to 14.2.12 and 14.2.13, show that (4) and (5) describe the waves, regardless of cross-sectional geometry. Note the relationship between G and C summarized by (7.6.4).
- 14.8.2** Although associated with the planar configuration of Fig. 14.8.1 in this section, the transmission line equations, (4) and (5), represent exact field solutions that are, in general, functions of the transverse coordinates as well as z . Thus, the transmission line represents a large family of exact solutions to Maxwell's equations. This follows from Prob. 14.8.1, where it is shown that the transmission line equations apply even if the regions between conductors are coaxial, as shown in Fig. 14.2.2b, with a material of uniform permittivity, permeability, and conductivity between $z = -l$ and $z = 0$. At $z = 0$, the transmission line conductors are "open circuit." At $z = -l$, the applied voltage is $\text{Re} \hat{V}_g \exp(j\omega t)$. Determine the electric and magnetic fields in the region between transmission line conductors. Include the dependence of the fields on the transverse coordinates. Note that the axial dependence of these fields is exactly as described in Examples 14.8.1 and 14.8.2.
- 14.8.3** The terminations and material between the conductors of a transmission line are as described in Prob. 14.8.2. However, rather than being coaxial, the perfectly conducting transmission line conductors are in the parallel wire configuration of Fig. 14.2.2a. In terms of $\Phi(x, y, z, t)$ and $A_z(x, y, z, t)$, determine the electric and magnetic fields over the length of the line, including their dependencies on the transverse coordinates. What are L , C , and G and hence β and Z_o ?
- 14.8.4*** The transmission line model for the strip line of Fig. 14.8.4a is derived in Prob. 14.1.1. Because the permittivity is not uniform over the cross-section of the line, the waves represented by the model are not exactly TEM. The approximation is valid as long as the wavelength is long enough so that (25)

is satisfied. In the approximation, E_x is taken as being uniform with x in each of the dielectrics, E^a and E^b , respectively. To estimate the longitudinal field E_z and compare it to E^a ,

- (a) Use the integral form of the law of induction applied to an incremental surface between $z + \Delta z$ and z and between the perfect conductors to derive Faraday's transmission line equation written in terms of E^a .

$$\left(a + \frac{\epsilon_a b}{\epsilon_b}\right) \frac{\partial E^a}{\partial z} = -\mu_o(a + b) \frac{\partial H_y}{\partial t} \quad (a)$$

- (b) Then carry out this same procedure using a surface that again has edges at $z + \Delta z$ and z on the upper perfect conductor, but which has its lower edge at the interface between dielectrics. With the axial electric field at the interface defined as E_z , show that

$$E_z = -a\mu_o \frac{\partial H_y}{\partial t} - a \frac{\partial E^a}{\partial z} = -ab\mu_o \frac{\left(\frac{\epsilon_a}{\epsilon_b} - 1\right)}{\left(a + \frac{\epsilon_a b}{\epsilon_b}\right)} \frac{\partial H_y}{\partial t} \quad (b)$$

- (c) Now show that in order for this field to be small compared to E^a , (25) must hold.

14.9 Quasi-One-Dimensional Models ($G = 0$)

- 14.9.1** The transmission line of Fig. 14.2.2a is comprised of wires having a finite conductivity σ , with the dielectric between of negligible conductivity. With the distribution of V and I described by (7) and (10), what are C , L , and R , and over what frequency range is this model valid? (Note Examples 4.6.3 and 8.6.1.) Give a condition on the dimensions $R \rightarrow a$ and l that must be satisfied to have the model be self-consistent over frequencies ranging from where the resistance dominates to where the inductive reactance dominates.
- 14.9.2** In the coaxial transmission line of Fig. 14.2.2b, the outer conductor has a thickness Δ . Each conductor has the conductivity σ . What are C , L , and R , and over what frequency range are (7) and (10) valid? Give a condition on the transverse dimensions that insures the model being valid into the frequency range where the inductive reactance dominates the resistance.
- 14.9.3** Find $V(z, t)$ on the charge diffusion line of Fig. 14.9.4 in the case where the applied voltage has been zero for $t < 0$ and suddenly becomes $V_p =$ constant for $0 < t$ and the line is shorted at $z = 0$. (Note Example 10.6.1.)
- 14.9.4** Find $V(z, t)$ under the conditions of Prob. 14.9.3 but with the line "open circuited" at $z = 0$.